

# High-precision VLBI astrometry of radio-emitting stars

J.-F. Lestrade<sup>1</sup>, R.A. Preston<sup>2</sup>, D.L. Jones<sup>2</sup>, R.B. Phillips<sup>3</sup>, A.E.E. Rogers<sup>3</sup>, M.A. Titus<sup>3</sup>, M.J. Rioja<sup>4</sup>, and D.C. Gabuzda<sup>5</sup>

<sup>1</sup> Observatoire de Paris-Meudon, URA-CNRS 1757, F-92195 Meudon Principal Cedex, France

<sup>2</sup> Jet Propulsion Laboratory, California Institute of Technology, 4800 Oak Grove Drive, Pasadena, CA 91109, USA

<sup>3</sup> Haystack Observatory, Massachusetts Institute of Technology, Route 40, Westford, Mass 01886, USA

<sup>4</sup> Joint Institute for VLBI in Europe JIVE, Postbus 2, 7990 AA Dwingeloo, The Netherlands

<sup>5</sup> Astro Space Center, Lebedev Physical Institute 53 Leninsky Prospekt, 117924 Moscow, Russia

Received 7 April 1998 / Accepted 5 November 1998

**Abstract.** Multiple-epoch phase-referenced VLBI observations of 11 radio-emitting stars have been conducted as part of an astrometric program to link the Hipparcos optical reference frame to the radio extragalactic reference frame. We present the VLBI positions, proper motions and trigonometric parallaxes from this program in the ICRF (International Celestial Reference Frame). These astrometric parameters are absolute because they are directly measured relative to the distant quasars used as VLBI phase reference calibrators. The mean astrometric precision achieved relative to the calibrators is 0.36 milliarcsecond and the highest precision is for the RS CVn close binary  $\sigma^2$  CrB with formal uncertainties of 0.12 milliarcsecond for its relative position, 0.05 milliarcsecond for its annual proper motion and 0.10 milliarcsecond for its trigonometric parallax.

In addition to the Hipparcos link, these observations have provided several new results. The distance to the nearby Tau-Auriga star forming region is  $148 \pm 5$  pc, determined directly through the VLBI trigonometric parallax of the Pre-Main-Sequence star HD283447 of this region. The orthogonality of the 2 orbital planes in the ternary system Algol is supported by new astrometric evidences. The proper motions of HR5110, HR1099 and IM Peg, regarded as possible guide stars for the NASA Gravity Probe B space mission, have formal precisions of 0.16, 0.31 and 0.40 milliarcsecond per year, respectively, and the mission requirement is 0.15 milliarcsecond per year. The close binary UX Ari is the only star that exhibits an acceleration larger than  $3\sigma$  and the most plausible cause is the gravitational interaction of a third body. The distances of the stars HD199178, IM Peg and AR Lac were uncertain by as much as 50% before our observations and are now  $116 \pm 4$ ,  $97 \pm 6$ ,  $41.7 \pm 0.6$  pc, respectively. The two X-ray binaries in our program, LSI61303 and Cyg X1, exhibit larger than expected post-fit position residuals. The linear scale of the rms of these residuals is  $> 10^{13}$  cm, more than 10 times the stellar separations in these systems. For LSI 61303, this scale is consistent with the size of the free-free absorption region of the enshrouding material beyond which radio radiation can escape. This would argue for *in situ* acceleration of the energetic electrons responsible for the synchrotron emission detected by VLBI as proposed by Vestrand (1983).

The space velocities of LSI 61303 and Cyg X1 determined with our VLBI proper motions, radial velocities and distances, are  $58 \pm 6$  and  $70 \pm 3$  km s<sup>-1</sup>, respectively, and are relatively high. This is expected if a neutron star or a black hole lurk in these systems.

**Key words:** techniques: interferometric – astrometry – reference systems – stars: binaries: general – stars: distances – radio continuum: stars

## 1. Introduction

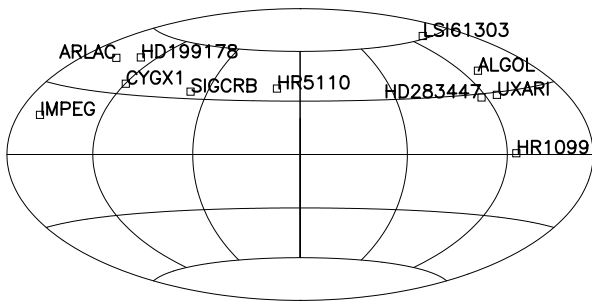
Astrometry of stars has a long history in optical astronomy. The measurement of positions, proper motions and trigonometric parallaxes of stars have important astrophysical implications, mainly for stellar structure and Galactic dynamics. The ESA Hipparcos astrometry space mission (Perryman 1989) has observed  $\sim 120\,000$  stars to provide their astrometric parameters with a precision of about 1 milliarcsecond (Kovalevsky et al. 1995, Lindegren & Kovalevsky 1995, Perryman et al. 1995). The best ground-based optical astrometry, however, has also reached milliarcsecond (mas) precision but on a limited number of stars (Monet et al. 1992, Gatewood et al. 1992, Tinney 1993, Hummel et al. 1995). At the same time, Very Long Baseline Interferometry (VLBI) has developed a radio celestial reference frame based on submilliarcsecond-precision coordinates of a few hundred distant radio quasars (Ma et al. 1990, Sovers 1991, Eubanks et al. 1991, Johnston et al. 1995). The VLBI extragalactic equatorial reference frame is the most precise and stable coordinate system ever materialized. The possible rotation rate of this extragalactic reference frame is estimated to be less than  $3 \times 10^{-9}$  "/yr following several theoretical assumptions and a variety of observations (Collins & Hawking 1973). This property makes it very suitable for dynamics studies and navigation of deep space probes in the Solar System.

The Hipparcos optical reference frame is not related to the equatorial reference frame nor the ecliptic reference frame. Consequently, it might have a sizeable residual rate of rotation with respect to distant quasars. In order to stop this residual rotation and to bring the optical and radio coordinate systems into co-

**Table 1.** Optical and spectroscopic properties of the 11 radio-emitting stars observed by VLBI for the Hipparcos link. Ten stars are in close binaries.

Star	Nature	Magnitude	Orbit diameter (mas)	Orbital Period (days)	Long-Orbit Period (years)	References
LSI61303	X-ray Binary	10.8 V	0.22	26.5	–	1
Algol	Algol Binary	2.9 V	2.2	2.9	1.86	2
UXAri	RSCVn Binary	7.3 P	1.72	6.5	–	3,4
HR1099	RSCVn Binary	6.7 P	1.48	2.8	2100	4
HD283447	PMS Binary	10.6 V	2.50	51.1	–	5
HR5110	RSCVn Binary	5.0 V	0.97	2.6	–	4
$\sigma^2$ CrB	RSCVn Binary	5.4 V	1.30	1.1	1000	4,6
Cyg X1	X-ray Binary	9.6 P	> 0.1	5.6	–	7
HD199178	Single Giant	8.3 P	–	–	–	–
AR Lac	RSCVn Binary	7.3 P	1.0	2.0	–	4
IM Peg	RSCVn Binary	5.7 V	> 1.0	24.6	–	4,8

References: (1) Taylor et al. 1992; (2) Söderhjelm 1980; (3) Carlos & Popper 1971; (4) Strassmeier et al. 1988; (5) Welty 1995; (6) Bakos 1984; (7) Hutchings et al. 1973; (8) Poe & Eaton 1985.

**Fig. 1.** Distribution of the 11 radio-emitting stars observed by VLBI.

incidence, a VLBI astrometric program of optically bright and radio-emitting stars was initiated in 1981 (Lestrade et al., 1982). The measurement of the positions and proper motions of these stars by both techniques (Hipparcos and VLBI) can be used to link the two coordinate systems together. This link was studied theoretically by Froeschlé & Kovalevsky (1982) and by Lindgren & Kovalevsky (1995) and a preliminary link based on the 30 month Hipparcos solution and the VLBI astrometric parameters of 7 radio stars was presented in Lestrade et al. (1995). The final alignment between the radio and optical frames has been determined with a precision of 0.5 mas at the epoch of the Hipparcos Catalog (1991.25) and of 0.3 mas/yr for the residual rotation rate by comparing the Hipparcos and VLBI parameters for 11 Northern stars and a Southern VLBI star (Lestrade et al. 1999 in preparation). In astrophysics, high angular resolution images made at optical wavelengths (e.g. Hubble) and at radio wavelengths (e.g. VLA) can now be registered at the level of a few milliarcseconds with this link and Galactic dynamics studies could be carried out relative to the non-rotating quasar reference frame.

The Hipparcos satellite required that stars be brighter than magnitude 10 to be observed in the best conditions and VLBI requires that the radio emission be non-thermal with brightness temperature in excess of  $10^8$  K. Non-thermal radio stars which are the site of synchrotron or gyro-synchrotron emission

processes (Dulk 1985) have highly variable radio flux densities exhibiting outbursts followed by quiescent periods on a large variety of time scales and magnitude ranges. We have selected the 11 radio-emitting stars of Table 1 for our multi-epoch VLBI astrometric observations because their low activity regime, *i.e.* radio quiescence, corresponds to a minimum flux density of 2 milliJansky (mJy), observable with VLBI by resorting to phase-referencing for enhanced sensitivity. The stars of Table 1 can be regarded as the most active non-thermal radio emitters which are also optically bright. Their peak flux densities during outbursts might be several hundred times their minimum quiescent flux density. In our sample, there are 6 RS CVn close binaries, 1 Algol type close binary (Algol itself), 2 X-ray binaries, 1 pre-main sequence star in a close binary and 1 single giant possibly of the FK Com type. Fig. 1 shows the distribution of these stars on the celestial sphere and Table 1 summarises their optical and spectroscopic properties. Three stars (Algol, HR1099,  $\sigma^2$  CrB) are part of a hierarchical ternary system with short and long period orbits. The diameters of the orbits are in Table 1 and are computed from  $\frac{a_1 \sin i + a_2 \sin i}{\sin i}$ , where  $a_1 \sin i$  and  $a_2 \sin i$  are the projected semi-major axis of the primary and secondary orbits directly measured by spectroscopy, and  $i$  is the inclination of the orbit relative to the sky. IM Peg is a single line spectroscopic binary and only  $a_1 \sin i$  is known. Orbit diameters will be used to compute source position jitters expected because of the binary morphology.

We present in this report the VLBI positions, annual proper motions and trigonometric parallaxes of the 11 radio-emitting stars of our Hipparcos/VLBI link program and discuss their precision that is formally below 1 mas. We also discuss some of the properties of each star in the light of these new astrometric measurements.

## 2. VLBI observations

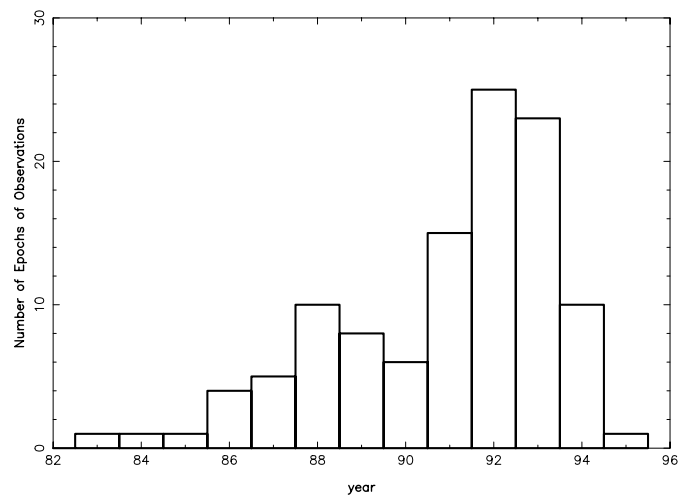
The 5 astrometric parameters of a star (right ascension, declination, 2 components of proper motion and trigonometric parallax) can be determined with measurements of its equatorial

**Table 2.** VLBI observations and reference sources

Star	Reference Source	Ref. source Flux density 8.4 GHz (Jansky)	Angular separation ( $^{\circ}$ )	Number of Observations	Observation Period
LSI61303	0241+622	0.3	0.60	9	89/09–95/05
Algol	0309+411	0.4	1.0	13	84/10–94/11
UXAri	0326+277	0.8	1.1	10	83/07–94/05
HR1099	CTA26	2.3	2.4	8	91/03 – 94/05
HD283447	0405+304	0.22	2.9	8	92/11–94/09
HD283447	0400+258	1.1	3.3	1	92/09–92/09
HR5110	OP326	0.25	4.5	9	87/05–94/05
HR5110	1338+381	0.15	1.5	7	92/09–94/05
$\sigma^2$ CrB	1611+343	2.9	0.5	14	87/05–94/11
Cyg X1	1955+335	0.25	1.6	7	88/03–93/11
HD199178	2100+468	0.14	2.9	6	92/09–94/09
AR Lac	BL Lac	3.0	3.7	7	89/04–94/05
IM Peg	3C454.3	10	0.75	4	91/12–94/07

coordinates at 3 epochs properly distributed over a year. For redundancy, we have conducted VLBI observations of the stars at a minimum of 4 epochs and up to 14 epochs. For each star, the number of VLBI observations and the period spanned by them are in Table 2. A total of 83 VLBI observing sessions were run for this program between 1983 and 1995 with three different VLBI arrays made of the combination of a very sensitive antenna (Phased-VLA (diameter = 130 m), Effelsberg (diameter = 100 m) or Goldstone DSS14(diameter = 70 m)) with smaller antennas of the 25 or 32 meter diameter class. Forty VLBI sessions were run using the Deep Space Network 70-meter radiotelescope (DSS14) at Goldstone as the primary station with three to four NRAO-VLBA antennas. Thirty nine VLBI sessions were run with the Global VLBI Network using the Phased-VLA and Effelsberg as the primary stations and four to five smaller antennas in the US and in Europe. Four VLBI sessions were run with the European VLBI Network (EVN) only including Effelsberg and three to four smaller antennas. Table 3 summarizes the antennas having participated in the 3 VLBI networks. The observing frequency was 5.0 GHz for 31 sessions on the global VLBI network and was 8.4 GHz for the rest when this frequency became the most sensitive on the Global VLBI Network after 1991. The distribution of the observations between 1983 and 1995 are shown in Fig. 2.

Each VLBI session was 5 to 15 hours long and was scheduled to observe one or two stars as switched observations between the star and its extragalactic reference source over a cycle of 5 minutes. The reference source was strong ( $> 100$  mJy) and angularly close to the star for high-precision differential astrometry and for enhancing the sensitivity of the array to make a 2 mJy source detectable. The total flux densities of the reference sources and their angular separations to the stars are in Table 2. For HD283447 and HR5110, two different reference sources were used in the course of the program as shown in Table 2. The raw VLBI data were recorded with the Mark III data acquisition system (Rogers et al. 1983). The bandwidth was 28 MHz at the rate of 56 Mbits/sec and the integration time was 2–3 minutes for each individual observation. The data were corre-

**Fig. 2.** Distribution of the VLBI observations with time

lated at Haystack Observatory (Mass) except for the four EVN only sessions that were correlated at the Max-Planck-Institut für Radioastronomie in Bonn (Germany).

### 3. Phase-referenced VLBI astrometry technique

Different approaches to differential astrometry using VLBI phase have been proposed and developed. The phase-connection approach (Shapiro et al. 1979) requires that all phases are unambiguously connected across the entire experiment for both the target and reference sources. This implies that the flux densities of both sources be strong enough to be directly detected by VLBI in individual observations of a few minutes at most. The phase-referenced mapping approach (Rogers 1989, Lestrade et al. 1990) corrects the visibilities of the target source with the reference source phase before the Fourier-inversion to produce a map of the radio brightness distribution with the source position information retained. This is similar to maps synthesized by connected-interferometry (e.g. VLA). The phase-referenced mapping technique requires phase connection only between the

**Table 3.** Radiotelescopes of the three VLBI arrays used.

Radiotelescope	Location	Diameter (m)	VLBI Network
DSS14 Goldstone	California	70	DSN-NRAO
Phased-VLA	New-Mexico	130	DSN-NRAO
Effelsberg	Germany	100	DSN-NRAO
Brewster (VLBA)	Washington State	25	DSN-NRAO
North Liberty (VLBA)	Iowa	25	DSN-NRAO
Fort Davis (VLBA)	Texas	25	DSN-NRAO
Hancock (VLBA)	New Hampshire	25	DSN-NRAO
Pie Town (VLBA)	New Mexico	25	DSN-NRAO
Los Alamos (VLBA)	Colorado	25	DSN-NRAO
Kitt Peak (VLBA)	Arizona	25	DSN-NRAO
Owens Valley (VLBA)	California	25	DSN-NRAO
Greenbank	West Virginia	43	Global VLBN
Haystack	Massachusetts	37	Global VLBN
OVRO	California	40	Global VLBN
Hat Creek	California	26	Global VLBN
Fort Davis/SAO	Texas	26	Global VLBN
Onsala	Sweeden	20	EVN
Medicina	Italy	32	EVN
Noto	Sicily (Italy)	32	EVN
Cambridge	England	32	EVN
Jodrell Bank Mk2	England	25	EVN

two consecutive observations of the reference source surrounding the star observation. So that long gaps in the observations might occur with no harm to the algorithm. In addition, since the connection of the target source phases is not required, the flux density of this source can be arbitrarily weak. This was important for the flux densities of the stars of our program that are typically in the 2–20 millijansky range. With such a low flux density, the fringe search of the target source must be carried out with constraints in single band delay and fringe rate that are readily available from the residual observables of the reference source if the *a priori* correlator model is accurate enough. This step might be called delay and delay-rate tracking of the weak star fringes. This strategy of observations is described in details and is applied to the star Algol with a flux density as low as 3 mJy in Lestrade et al. 1990.

#### 4. Analysis

For this project, we have developed a specific software named SPRINT (Software for Phase Referenced INTerferometry) that uses as input the total phase delay and phase delay rate yielded by the cross-correlation of the recorded VLBI data after the correlator model has been restored. First, SPRINT computes new phase and delay rate residuals with a high-accuracy delay model in which only the relative separation between the target and reference sources must be refined. Then, SPRINT uses a scheme to interpolate the reference source phase at the times of the interleaved observations of the star, constructs differenced residual phases at these times, and makes a Fourier inversion of the referenced star visibilities. Various phase interpolation

schemes can be selected in SPRINT. The final relative position between the star and the reference source is directly measured from the ‘dirty’ phase-referenced map. An example of such a map as well as the point-source response of the VLBI array are given in Fig. 3. This phase-referenced map is typical of most of the ones we have produced from the VLBI observations of our program. The SNR at the map peak is 34 in Fig. 3. The relatively high side lobes in this map are not a limiting factor for astrometry of point-like sources and could be largely removed by the CLEAN algorithm for better representing the source structure.

The high-accuracy model in SPRINT is based on the description of the VLBI delay model by Sovers & Jacobs (1996) but small effects have been ignored because they are negligible for differential astrometry over a few degree separation. The main characteristics of the SPRINT model are that it includes the IAU 1980 Wahr Nutation series for the relationship between the terrestrial and celestial reference frames, the solid-Earth tidal motion of stations, the Special Relativity aberration effect, the general relativity Shapiro delay, the dry and wet tropospheric zenith delays computed with meteorological data (Saastamoinen 1973) and the Chao mapping function, and the ionospheric phase delay modeled with the seasonally averaged total electronic content of Klobuchar (1975). The geometric delay of equatorial or azimuth-elevation antenna mounts with non-zero axis offset is modeled as well as the phase delay of the feed rotation.

For this analysis, we have adopted the terrestrial reference frame of the International Earth Rotation Service (IERS) (Boucher et al. 1993) including station coordinates and velocities. The coordinates of the radiotelescopes (Table 3) have centimeter level precision at epoch 1988, except for the VLA phase-center which has reduced precision of  $\sim 20$  cm. We have adopted the International Celestial Reference Frame (ICRF) (Ma et al. 1998) which is materialized in our analysis by the coordinates of the 13 reference sources in Table 4. Consistently, we have adopted the IERS series for the Earth Orientation Parameters and corrections ( $\Delta\phi$ ,  $\Delta\epsilon$ ) to the IAU 1980 Nutation. The ICRF coordinates of the reference sources were determined through the joint effort of VLBI groups at Goddard Space Flight Center, Jet Propulsion Laboratory, US Naval Observatory and the Central Bureau of IERS for the Hipparcos link.

In the present analysis, the structure phases of the reference sources have not been modeled for lack of appropriate VLBI maps at the epochs of observations. However, the structure of each reference source was examined with at least a single-epoch VLBI map found in the literature or made with our data. The reference source 1338+381 for the star HR5110 is the most pathological case having two main components with flux density ratio varying from 0.5 to  $\sim 1$  and with a separation of  $\sim 4$  mas between 1992 and 1994 (Bouchy et al. 1998). Several tests using VLBI maps and the software for computation of structure effects in VLBI observables developed by Charlot (1990) indicate that the resulting systematic bias in the position of the star at each epoch of observation is less than 1 mas, in general, but reached 2.2 mas in May 1994 for HR5110 with the reference source 1338+381 (Bouchy 1995). A VLBI map of the reference quasar

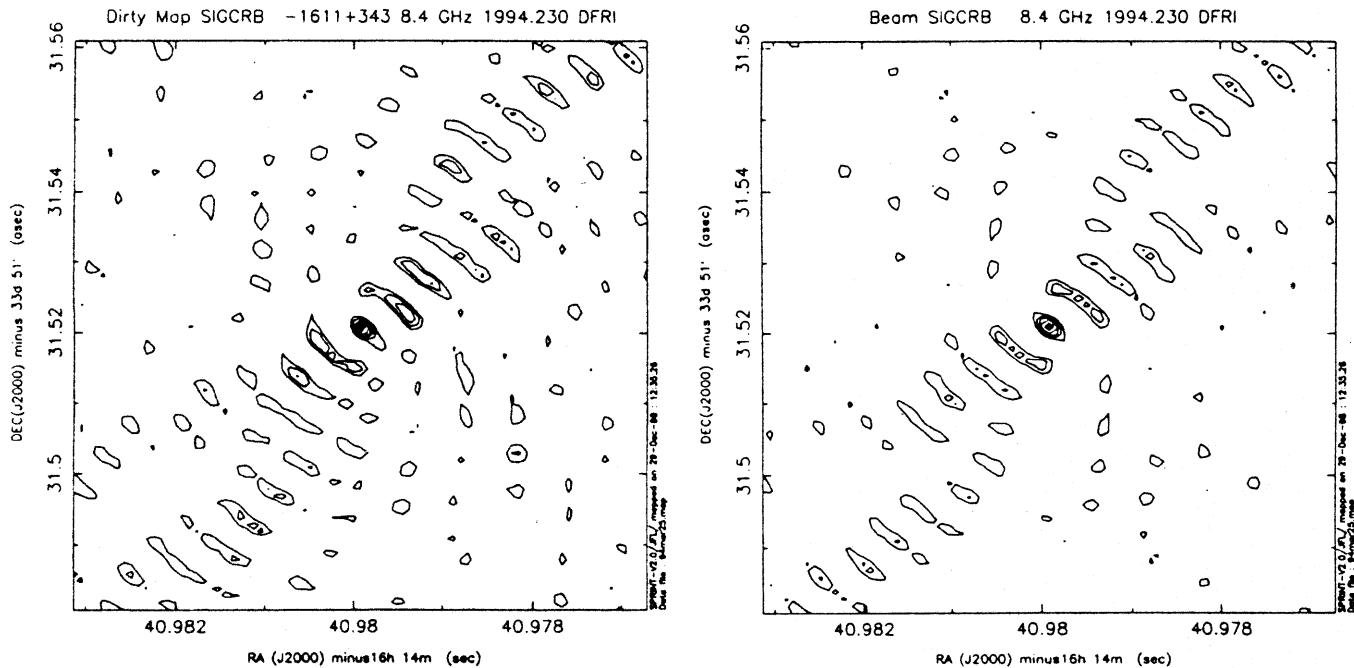


**Fig. 3.** UNCLEANed phase-referenced map (“dirty map”) and point source response map (“beam”) of  $\sigma^2$  CrB observed at 8.4 GHz on 1994 March 25th with the VLBI array composed with Goldstone and the VLBA antennas at Brewster, North Liberty and Fort Davis. Contours are 20, 35, 50, 65, 80, 85, 90, 95, 99% of peak.

**Table 4.** ICRF VLBI coordinates of the reference extragalactic radio sources (Ma et al. 1998).

Extragalactic source	$\alpha$ (J2000) (h m s)	$\delta$ (J2000) ( $^{\circ}$ ' ")
0241+622	02 44 57.696828 $\pm$ 0.000425	+62 28 06.51494 $\pm$ 0.00185
0309+411	03 13 01.962129 $\pm$ 0.000026	+41 20 01.18353 $\pm$ 0.00031
0326+277	03 29 57.669425 $\pm$ 0.000138	+27 56 15.49901 $\pm$ 0.00210
CTA26	03 39 30.937785 $\pm$ 0.000017	-01 46 35.80391 $\pm$ 0.00026
0400+258	04 03 05.586048 $\pm$ 0.000020	+26 00 01.50274 $\pm$ 0.00030
0405+304	04 08 20.377574 $\pm$ 0.000201	+30 32 30.49043 $\pm$ 0.00512
OP326	13 17 36.494181 $\pm$ 0.000025	+34 25 15.93257 $\pm$ 0.00049
1338+381	13 40 22.951763 $\pm$ 0.000111	+37 54 43.83468 $\pm$ 0.00120
1611+343	16 13 41.064250 $\pm$ 0.000021	+34 12 47.90905 $\pm$ 0.00026
1955+335	19 57 40.550036 $\pm$ 0.000099	+33 38 27.94555 $\pm$ 0.00148
2100+468	21 02 17.056050 $\pm$ 0.000181	+47 02 16.25468 $\pm$ 0.00193
BL LAC	22 02 43.291381 $\pm$ 0.000066	+42 16 39.97998 $\pm$ 0.00087
3C454.3	22 53 57.747938 $\pm$ 0.000079	+16 08 53.56088 $\pm$ 0.00137

made at each epoch of observation could greatly alleviate this source of systematic error in the future. The structure of the radio-emitting region of the star is equally important and an area where improvement is expected in the future.

The switched observations between the target and reference sources we conducted required that the residual phases of the reference source be extrapolated to the times of observations of the target star. We have used various schemes for this extrapolation and found very similar results. One scheme, named *double linear extrapolation* in SPRINT, is based on the fact that the residual delay rates of the reference source are usually dominated by the fluctuations of the atmosphere of  $\sim 10^{-13}$  s/s. Such a rate is low enough that there is no  $2\pi$  ambiguity in the phase

at 8.4 GHz between consecutive observations of the reference source for switching cycle time of a few minutes. So it is possible to extrapolate forward and backward the residual phases of the reference source by using its residual delay rates from the two observations surrounding an observation of the star. The mean of these two extrapolated phases can be used for the reference source phase at the time of observation of the target star. The rms of the differences between the forward and backward extrapolated phases were between  $40^{\circ}$  and  $60^{\circ}$  for the VLBI sessions in our program. Another scheme, named *Phase Connection* in SPRINT, is based on the linear interpolation of the two reference source phases surrounding the star observation after resolving the  $2\pi$  ambiguity, if any, with the residual delay

rates. Note that these two schemes are not affected by possible long gaps in the observations. The second scheme should, in principle, be better than the first one because any slip of the reference phase larger than  $2\pi$  will be accounted for properly with the phase connection option but erroneously with the double linear interpolation option. We found negligible differences in the positions of the stars of our program between these two options. This implies that the VLBI arrays we used were phase stable over the switching cycle.

We have studied possible systematic errors in the relative coordinates of the stars measured from the SPRINT phase-referenced maps. These errors arise from uncertainties in the station coordinates, reference source coordinates, Earth Orientation Parameters and by imperfect modeling of the troposphere and ionosphere. The wet zenith component of the troposphere might be in error by about 10 cm while the dry component should be accurate to better than 2 cm. The ionosphere model uses the seasonally averaged model of Klobuchar (1975) and might be in error by 100% (i.e. 3 cm at 5 GHz and 1 cm at 8.4 GHz). This study essentially confirms the result we already obtained that systematic position error is  $\sim 0.15$  mas at 5 GHz (see Table 3 in Lestrade et al. 1990) and  $\sim 0.12$  mas at 8.4 GHz for an angular separation of  $1^\circ$  between the reference and target sources with VLBI arrays composed of baselines ranging from 1000 to 4000 km described in Sect. 2. This position error scales linearly with angular separation.

## 5. VLBI astrometric results

For each star, we have solved for 7 VLBI astrometric parameters (relative coordinates at epoch; proper motion and acceleration components and trigonometric parallax) by a Least-Squares-fit of the VLBI coordinates measured at multiple epochs. Separate fits were also made without the acceleration parameters. These astrometric parameters are defined by the two relations:

$$\begin{aligned} \cos \delta_0 \Delta \alpha(t_j) &= \cos \delta_0 \Delta \alpha_0 + \cos \delta_0 \mu_\alpha (t_j - t_0) \\ &+ \frac{1}{2} \cos \delta_0 \gamma_\alpha (t_j - t_0)^2 \\ &+ \pi [R_x(t_j) \times \sin \alpha_0 - R_y(t_j) \times \cos \alpha_0] \end{aligned}$$

$$\begin{aligned} \Delta \delta(t_j) &= \Delta \delta_0 + \mu_\delta (t_j - t_0) + \frac{1}{2} \gamma_\delta (t_j - t_0)^2 \\ &+ \pi [\sin \delta_0 (R_x(t_j) \times \cos \alpha_0 + R_y(t_j) \times \sin \alpha_0) \\ &- R_z(t_j) \times \cos \delta_0] \end{aligned}$$

where  $\Delta \alpha_0$  and  $\Delta \delta_0$  are the coordinates of the star at epoch  $t_0$  relative to the reference source,  $\mu_\alpha$  and  $\mu_\delta$  are the proper motion components,  $\gamma_\alpha$  and  $\gamma_\delta$  are the acceleration components,  $\pi$  is the trigonometric parallax and  $R_x(t_j)$ ,  $R_y(t_j)$ ,  $R_z(t_j)$  are the equatorial barycentric coordinates of the earth in AU at the time of observation  $t_j$ . As discussed in Van de Kamp 1981 (p. 59), with increasing precision in astrometry, barycentric coordinates of the Earth rather than heliocentric coordinates must be used to provide time-invariant parallaxes. These equations are limited to first order in  $\mu$ ,  $\pi$  and  $\gamma$  and the perspective secular acceleration ( $\frac{d\mu}{dt} \propto V_R \mu \pi$ ; van de Kamp 1981, p.50) depending on the

radial velocity  $V_R$  is not included in the equation above but is  $\leq 10^{-7}''/\text{yr}^2$  for the stars of our program.

Table 5 summarises the VLBI astrometric results. This table includes the position of each star relative to its reference source as directly determined from the phase-referenced VLBI observations. Also provided in this table are the absolute coordinates of the star after adding the reference source ICRF coordinates listed in Table 4. Coordinates are provided at date of observation in the ICRF. Note that proper motion and parallax are absolute because they are directly measured relative to distant quasars. For Algol, the astrometric parameters reported in this table are for the mass center of the ternary system when the 1.86 yr period orbit is modeled with the elements and mass ratios from Söderjhem (1980).

The formal uncertainties of the relative position, proper motion and trigonometric parallax in Table 5 are obtained by tweaking the measurement uncertainties to make the normalized goodness of fit  $\chi^2$  unity following standard practice in VLBI astrometry. For each star, we have assigned the same tweaked measurement uncertainty to all epochs of observations since there has been no evidence for the position precision to depend on the signal-to-noise ratio that ranges from 10 to a few hundreds according to the level of activity of the star. For the highest signal-to-noise ratio, the theoretical uncertainties from SPRINT were smaller than  $10 \mu\text{as}$ . This is unrealistically small and the empirically determined uncertainties range from 0.35 to 1.5 mas according to the star. They are compared in Table 6 to the VLBI systematic errors estimated in Sect. 4 and linearly scaled with the angular separation between the reference and target sources.

The uncertainty of the absolute position of a star in Table 5 is the quadratically combined uncertainties of the star relative position and of the reference source position of Table 4. Note that two reference sources only (0309+411 and 0400+258) are part of the 212 defining sources of the ICRF (Ma et al. 1998) while most of the others are candidate sources in the ICRF and their coordinates will be improved. The high-precision relative position of the stars provided in Table 5 could be added to these new coordinates when available.

In Table 6, also for comparison, the orbital jitter  $\sqrt{\sum_{j=1}^n (a \cos \phi(t_j))^2 / n}$  is calculated with  $a$ , the semi-major axis of the binary orbit, and  $\phi(t_j)$ , the orbital phase at time  $t_j$  of observation. This calculation of the orbital jitter assumes that the radio-emitting region is bound to the photosphere of one of the star of the binary modulating its radio position. In general, the post-fit rms of Table 6 (Column 1) are not dominated by the VLBI systematic errors (Column 2) but are commensurable with the orbital jitters (Column 3) that appear to be the largest source of error in our measurements. This indicates that the apparent stellar source structure variations caused by the orbital jitter are limiting the astrometric precision. HD283447 and  $\sigma^2$  CrB are exceptions since their post-fit rms are smaller than the orbital jitter and this may indicate that the radio-emitting region is not bound to the photospheres of the stars but are associated with the intra-stellar regions of these binaries (Lestrade 1996). Finally, a

**Table 5.** Table 5: VLBI astrometric parameters of the 11 radio-emitting stars of the Hipparcos/VLBI link program. The differential coordinates  $\Delta\alpha$  and  $\Delta\delta$  are determined relative to the reference source directly by our phase-referenced VLBI observations. They are given in the ICRF at the dates listed in the second column. The absolute right ascension and declination  $\alpha$  and  $\delta$  are computed by adding  $\Delta\alpha$  and  $\Delta\delta$  to the ICRF VLBI coordinates (Table 4) of the reference source indicated in parenthesis. The other parameters are the 2 components of the proper motion  $\mu_\alpha$  and  $\mu_\delta$ , the 2 components of the acceleration  $\gamma_\alpha$  and  $\gamma_\delta$  and the trigonometric parallax  $\pi$ . The uncertainties for  $\alpha$ ,  $\mu_\alpha$  and  $\gamma_\alpha$  have not been multiplied by  $\cos \delta$ . For Algol, the astrometric parameters given are for the mass center of the ternary system (see text of Sect. 5).

Star (Reference)	Epoch	$\Delta\alpha$ (J2000) (h m s) $\alpha$ (J2000) (h m s) $\mu_\alpha$ (sec/yr) $\gamma_\alpha$ (sec/yr <sup>2</sup> )	$\Delta\delta$ (J2000) (° ' ") $\delta$ (J2000) (° ' ") $\mu_\delta$ ("/yr) $\gamma_\delta$ ("/yr <sup>2</sup> )	Trigon. parallax $\pi$ (mas)	Post-fit rms (mas)	Deg of freed																																																																																																											
$\Delta$ -LSI61303	920101	-00 04 26.032334 $\pm$ 0.000035	-01 14 20.91892 $\pm$ 0.00056	0.26 $\pm$ 0.61	1.25	13																																																																																																											
LSI61303 (0241+622)	920101	02 40 31.664494 $\pm$ 0.000426 +0.000134 $\pm$ 0.000036 < 0.00008	61 13 45.59602 $\pm$ 0.00193 -0.00121 $\pm$ 0.00032 < 0.00042				$\Delta$ -ALGOL	890413	-00 04 51.832826 $\pm$ 0.000035	-00 22 40.83840 $\pm$ 0.00052	33.32 $\pm$ 0.73 40 57 20.34513 $\pm$ 0.00061	1.24	21	ALGOL (0309+411)	890413	03 08 10.129303 $\pm$ 0.000044 +0.000246 $\pm$ 0.000012 < 0.000006	03 08 10.129303 $\pm$ 0.000044 -0.00064 $\pm$ 0.00018 < 0.00004	$\Delta$ -UX Ari	910401	-00 03 22.308032 $\pm$ 0.000024	00 46 39.72604 $\pm$ 0.00036	19.37 $\pm$ 0.39	0.83	13	UX Ari (0326+277)	910401	03 26 35.361393 $\pm$ 0.000140 +0.003134 $\pm$ 0.000014 -0.000041 $\pm$ 0.000005	28 42 55.22505 $\pm$ 0.00213 -0.10401 $\pm$ 0.00020 -0.00029 $\pm$ 0.00007	$\Delta$ -HR1099	920101	-00 02 43.630576 $\pm$ 0.000027	00 21 53.04026 $\pm$ 0.00040	33.88 $\pm$ 0.47	0.84	11	HR1099 (CTA26)	920101	03 36 47.307209 $\pm$ 0.000032 -0.002106 $\pm$ 0.000022 < 0.000043	00 35 17.23635 $\pm$ 0.00048 -0.16169 $\pm$ 0.00031 < 0.00052	$\Delta$ -HD283447	931118	00 05 52.541931 $\pm$ 0.000015	-02 20 18.05114 $\pm$ 0.00020	6.74 $\pm$ 0.25	0.57	13	HD283447 (0405+304)	931118	04 14 12.919505 $\pm$ 0.000201 0.000032 $\pm$ 0.000022 < 0.00006	28 12 12.43929 $\pm$ 0.00512 -0.02325 $\pm$ 0.00028 < 0.0014	$\Delta$ -HR5110	930209	00 17 11.265295 $\pm$ 0.000031	02 45 40.82758 $\pm$ 0.00045	22.21 $\pm$ 0.45	1.38	27	HR5110 (OP326)	930209	13 34 47.759476 $\pm$ 0.000040 +0.007154 $\pm$ 0.000011 < 0.0000013	37 10 56.76015 $\pm$ 0.00067 -0.00922 $\pm$ 0.00016 < 0.00057	$\Delta$ - $\sigma^2$ CrB	900101	00 01 00.003262 $\pm$ 0.000008	-00 21 16.03486 $\pm$ 0.00012	43.93 $\pm$ 0.10	0.32	23	$\sigma^2$ CrB (1611+343)	900101	16 14 41.067512 $\pm$ 0.000022 -0.021439 $\pm$ 0.000003 < 0.0000033	33 51 31.87419 $\pm$ 0.00029 -0.08666 $\pm$ 0.00005 < 0.00001	$\Delta$ -Cyg X1	910402	00 00 41.128564 $\pm$ 0.000022	01 33 37.89682 $\pm$ 0.00032	0.73 $\pm$ 0.30	0.59	7	Cyg X1 (1955+335)	910402	19 58 21.678600 $\pm$ 0.000101 -0.000309 $\pm$ 0.000014 < 0.0000093	35 12 05.84237 $\pm$ 0.00175 -0.00625 $\pm$ 0.00021 < 0.00015	$\Delta$ -HD199178	931017	-00 08 23.419214 $\pm$ 0.000017	-02 39 05.16806 $\pm$ 0.00026	8.59 $\pm$ 0.33	0.37	7	HD199178 (2100+468)	931017	20 53 53.636836 $\pm$ 0.000182 +0.002481 $\pm$ 0.000038 < 0.00017	44 23 11.08662 $\pm$ 0.00195 -0.00124 $\pm$ 0.00043 < 0.0014	$\Delta$ -AR Lac	920608	00 05 57.564529 $\pm$ 0.000026	03 27 51.77158 $\pm$ 0.00036	23.97 $\pm$ 0.37	0.66	9	AR Lac (BL Lac)	920608	22 08 40.855910 $\pm$ 0.000071 -0.004975 $\pm$ 0.000012 < 0.0000067	45 44 31.75156 $\pm$ 0.00094 +0.04703 $\pm$ 0.00019 < 0.0002	$\Delta$ -IM Peg	921201	-00 00 55.471694 $\pm$ 0.000025	00 41 34.93142 $\pm$ 0.00039	10.28 $\pm$ 0.62	0.38	3	IM Peg (3C454.4)
$\Delta$ -ALGOL	890413	-00 04 51.832826 $\pm$ 0.000035	-00 22 40.83840 $\pm$ 0.00052	33.32 $\pm$ 0.73 40 57 20.34513 $\pm$ 0.00061	1.24	21																																																																																																											
ALGOL (0309+411)	890413	03 08 10.129303 $\pm$ 0.000044 +0.000246 $\pm$ 0.000012 < 0.000006	03 08 10.129303 $\pm$ 0.000044 -0.00064 $\pm$ 0.00018 < 0.00004				$\Delta$ -UX Ari	910401	-00 03 22.308032 $\pm$ 0.000024	00 46 39.72604 $\pm$ 0.00036	19.37 $\pm$ 0.39	0.83	13	UX Ari (0326+277)	910401	03 26 35.361393 $\pm$ 0.000140 +0.003134 $\pm$ 0.000014 -0.000041 $\pm$ 0.000005	28 42 55.22505 $\pm$ 0.00213 -0.10401 $\pm$ 0.00020 -0.00029 $\pm$ 0.00007	$\Delta$ -HR1099	920101	-00 02 43.630576 $\pm$ 0.000027	00 21 53.04026 $\pm$ 0.00040	33.88 $\pm$ 0.47	0.84	11	HR1099 (CTA26)	920101	03 36 47.307209 $\pm$ 0.000032 -0.002106 $\pm$ 0.000022 < 0.000043	00 35 17.23635 $\pm$ 0.00048 -0.16169 $\pm$ 0.00031 < 0.00052	$\Delta$ -HD283447	931118	00 05 52.541931 $\pm$ 0.000015	-02 20 18.05114 $\pm$ 0.00020	6.74 $\pm$ 0.25	0.57	13	HD283447 (0405+304)	931118	04 14 12.919505 $\pm$ 0.000201 0.000032 $\pm$ 0.000022 < 0.00006	28 12 12.43929 $\pm$ 0.00512 -0.02325 $\pm$ 0.00028 < 0.0014	$\Delta$ -HR5110	930209	00 17 11.265295 $\pm$ 0.000031	02 45 40.82758 $\pm$ 0.00045	22.21 $\pm$ 0.45	1.38	27	HR5110 (OP326)	930209	13 34 47.759476 $\pm$ 0.000040 +0.007154 $\pm$ 0.000011 < 0.0000013	37 10 56.76015 $\pm$ 0.00067 -0.00922 $\pm$ 0.00016 < 0.00057	$\Delta$ - $\sigma^2$ CrB	900101	00 01 00.003262 $\pm$ 0.000008	-00 21 16.03486 $\pm$ 0.00012	43.93 $\pm$ 0.10	0.32	23	$\sigma^2$ CrB (1611+343)	900101	16 14 41.067512 $\pm$ 0.000022 -0.021439 $\pm$ 0.000003 < 0.0000033	33 51 31.87419 $\pm$ 0.00029 -0.08666 $\pm$ 0.00005 < 0.00001	$\Delta$ -Cyg X1	910402	00 00 41.128564 $\pm$ 0.000022	01 33 37.89682 $\pm$ 0.00032	0.73 $\pm$ 0.30	0.59	7	Cyg X1 (1955+335)	910402	19 58 21.678600 $\pm$ 0.000101 -0.000309 $\pm$ 0.000014 < 0.0000093	35 12 05.84237 $\pm$ 0.00175 -0.00625 $\pm$ 0.00021 < 0.00015	$\Delta$ -HD199178	931017	-00 08 23.419214 $\pm$ 0.000017	-02 39 05.16806 $\pm$ 0.00026	8.59 $\pm$ 0.33	0.37	7	HD199178 (2100+468)	931017	20 53 53.636836 $\pm$ 0.000182 +0.002481 $\pm$ 0.000038 < 0.00017	44 23 11.08662 $\pm$ 0.00195 -0.00124 $\pm$ 0.00043 < 0.0014	$\Delta$ -AR Lac	920608	00 05 57.564529 $\pm$ 0.000026	03 27 51.77158 $\pm$ 0.00036	23.97 $\pm$ 0.37	0.66	9	AR Lac (BL Lac)	920608	22 08 40.855910 $\pm$ 0.000071 -0.004975 $\pm$ 0.000012 < 0.0000067	45 44 31.75156 $\pm$ 0.00094 +0.04703 $\pm$ 0.00019 < 0.0002	$\Delta$ -IM Peg	921201	-00 00 55.471694 $\pm$ 0.000025	00 41 34.93142 $\pm$ 0.00039	10.28 $\pm$ 0.62	0.38	3	IM Peg (3C454.4)	921201	22 53 02.276244 $\pm$ 0.000083 -0.001434 $\pm$ 0.000032 < 0.000027	16 50 28.49230 $\pm$ 0.00142 -0.02753 $\pm$ 0.00040 < 0.0015								
$\Delta$ -UX Ari	910401	-00 03 22.308032 $\pm$ 0.000024	00 46 39.72604 $\pm$ 0.00036	19.37 $\pm$ 0.39	0.83	13																																																																																																											
UX Ari (0326+277)	910401	03 26 35.361393 $\pm$ 0.000140 +0.003134 $\pm$ 0.000014 -0.000041 $\pm$ 0.000005	28 42 55.22505 $\pm$ 0.00213 -0.10401 $\pm$ 0.00020 -0.00029 $\pm$ 0.00007				$\Delta$ -HR1099	920101	-00 02 43.630576 $\pm$ 0.000027	00 21 53.04026 $\pm$ 0.00040	33.88 $\pm$ 0.47	0.84	11	HR1099 (CTA26)	920101	03 36 47.307209 $\pm$ 0.000032 -0.002106 $\pm$ 0.000022 < 0.000043	00 35 17.23635 $\pm$ 0.00048 -0.16169 $\pm$ 0.00031 < 0.00052	$\Delta$ -HD283447	931118	00 05 52.541931 $\pm$ 0.000015	-02 20 18.05114 $\pm$ 0.00020	6.74 $\pm$ 0.25	0.57	13	HD283447 (0405+304)	931118	04 14 12.919505 $\pm$ 0.000201 0.000032 $\pm$ 0.000022 < 0.00006	28 12 12.43929 $\pm$ 0.00512 -0.02325 $\pm$ 0.00028 < 0.0014	$\Delta$ -HR5110	930209	00 17 11.265295 $\pm$ 0.000031	02 45 40.82758 $\pm$ 0.00045	22.21 $\pm$ 0.45	1.38	27	HR5110 (OP326)	930209	13 34 47.759476 $\pm$ 0.000040 +0.007154 $\pm$ 0.000011 < 0.0000013	37 10 56.76015 $\pm$ 0.00067 -0.00922 $\pm$ 0.00016 < 0.00057	$\Delta$ - $\sigma^2$ CrB	900101	00 01 00.003262 $\pm$ 0.000008	-00 21 16.03486 $\pm$ 0.00012	43.93 $\pm$ 0.10	0.32	23	$\sigma^2$ CrB (1611+343)	900101	16 14 41.067512 $\pm$ 0.000022 -0.021439 $\pm$ 0.000003 < 0.0000033	33 51 31.87419 $\pm$ 0.00029 -0.08666 $\pm$ 0.00005 < 0.00001	$\Delta$ -Cyg X1	910402	00 00 41.128564 $\pm$ 0.000022	01 33 37.89682 $\pm$ 0.00032	0.73 $\pm$ 0.30	0.59	7	Cyg X1 (1955+335)	910402	19 58 21.678600 $\pm$ 0.000101 -0.000309 $\pm$ 0.000014 < 0.0000093	35 12 05.84237 $\pm$ 0.00175 -0.00625 $\pm$ 0.00021 < 0.00015	$\Delta$ -HD199178	931017	-00 08 23.419214 $\pm$ 0.000017	-02 39 05.16806 $\pm$ 0.00026	8.59 $\pm$ 0.33	0.37	7	HD199178 (2100+468)	931017	20 53 53.636836 $\pm$ 0.000182 +0.002481 $\pm$ 0.000038 < 0.00017	44 23 11.08662 $\pm$ 0.00195 -0.00124 $\pm$ 0.00043 < 0.0014	$\Delta$ -AR Lac	920608	00 05 57.564529 $\pm$ 0.000026	03 27 51.77158 $\pm$ 0.00036	23.97 $\pm$ 0.37	0.66	9	AR Lac (BL Lac)	920608	22 08 40.855910 $\pm$ 0.000071 -0.004975 $\pm$ 0.000012 < 0.0000067	45 44 31.75156 $\pm$ 0.00094 +0.04703 $\pm$ 0.00019 < 0.0002	$\Delta$ -IM Peg	921201	-00 00 55.471694 $\pm$ 0.000025	00 41 34.93142 $\pm$ 0.00039	10.28 $\pm$ 0.62	0.38	3	IM Peg (3C454.4)	921201	22 53 02.276244 $\pm$ 0.000083 -0.001434 $\pm$ 0.000032 < 0.000027	16 50 28.49230 $\pm$ 0.00142 -0.02753 $\pm$ 0.00040 < 0.0015																			
$\Delta$ -HR1099	920101	-00 02 43.630576 $\pm$ 0.000027	00 21 53.04026 $\pm$ 0.00040	33.88 $\pm$ 0.47	0.84	11																																																																																																											
HR1099 (CTA26)	920101	03 36 47.307209 $\pm$ 0.000032 -0.002106 $\pm$ 0.000022 < 0.000043	00 35 17.23635 $\pm$ 0.00048 -0.16169 $\pm$ 0.00031 < 0.00052				$\Delta$ -HD283447	931118	00 05 52.541931 $\pm$ 0.000015	-02 20 18.05114 $\pm$ 0.00020	6.74 $\pm$ 0.25	0.57	13	HD283447 (0405+304)	931118	04 14 12.919505 $\pm$ 0.000201 0.000032 $\pm$ 0.000022 < 0.00006	28 12 12.43929 $\pm$ 0.00512 -0.02325 $\pm$ 0.00028 < 0.0014	$\Delta$ -HR5110	930209	00 17 11.265295 $\pm$ 0.000031	02 45 40.82758 $\pm$ 0.00045	22.21 $\pm$ 0.45	1.38	27	HR5110 (OP326)	930209	13 34 47.759476 $\pm$ 0.000040 +0.007154 $\pm$ 0.000011 < 0.0000013	37 10 56.76015 $\pm$ 0.00067 -0.00922 $\pm$ 0.00016 < 0.00057	$\Delta$ - $\sigma^2$ CrB	900101	00 01 00.003262 $\pm$ 0.000008	-00 21 16.03486 $\pm$ 0.00012	43.93 $\pm$ 0.10	0.32	23	$\sigma^2$ CrB (1611+343)	900101	16 14 41.067512 $\pm$ 0.000022 -0.021439 $\pm$ 0.000003 < 0.0000033	33 51 31.87419 $\pm$ 0.00029 -0.08666 $\pm$ 0.00005 < 0.00001	$\Delta$ -Cyg X1	910402	00 00 41.128564 $\pm$ 0.000022	01 33 37.89682 $\pm$ 0.00032	0.73 $\pm$ 0.30	0.59	7	Cyg X1 (1955+335)	910402	19 58 21.678600 $\pm$ 0.000101 -0.000309 $\pm$ 0.000014 < 0.0000093	35 12 05.84237 $\pm$ 0.00175 -0.00625 $\pm$ 0.00021 < 0.00015	$\Delta$ -HD199178	931017	-00 08 23.419214 $\pm$ 0.000017	-02 39 05.16806 $\pm$ 0.00026	8.59 $\pm$ 0.33	0.37	7	HD199178 (2100+468)	931017	20 53 53.636836 $\pm$ 0.000182 +0.002481 $\pm$ 0.000038 < 0.00017	44 23 11.08662 $\pm$ 0.00195 -0.00124 $\pm$ 0.00043 < 0.0014	$\Delta$ -AR Lac	920608	00 05 57.564529 $\pm$ 0.000026	03 27 51.77158 $\pm$ 0.00036	23.97 $\pm$ 0.37	0.66	9	AR Lac (BL Lac)	920608	22 08 40.855910 $\pm$ 0.000071 -0.004975 $\pm$ 0.000012 < 0.0000067	45 44 31.75156 $\pm$ 0.00094 +0.04703 $\pm$ 0.00019 < 0.0002	$\Delta$ -IM Peg	921201	-00 00 55.471694 $\pm$ 0.000025	00 41 34.93142 $\pm$ 0.00039	10.28 $\pm$ 0.62	0.38	3	IM Peg (3C454.4)	921201	22 53 02.276244 $\pm$ 0.000083 -0.001434 $\pm$ 0.000032 < 0.000027	16 50 28.49230 $\pm$ 0.00142 -0.02753 $\pm$ 0.00040 < 0.0015																														
$\Delta$ -HD283447	931118	00 05 52.541931 $\pm$ 0.000015	-02 20 18.05114 $\pm$ 0.00020	6.74 $\pm$ 0.25	0.57	13																																																																																																											
HD283447 (0405+304)	931118	04 14 12.919505 $\pm$ 0.000201 0.000032 $\pm$ 0.000022 < 0.00006	28 12 12.43929 $\pm$ 0.00512 -0.02325 $\pm$ 0.00028 < 0.0014				$\Delta$ -HR5110	930209	00 17 11.265295 $\pm$ 0.000031	02 45 40.82758 $\pm$ 0.00045	22.21 $\pm$ 0.45	1.38	27	HR5110 (OP326)	930209	13 34 47.759476 $\pm$ 0.000040 +0.007154 $\pm$ 0.000011 < 0.0000013	37 10 56.76015 $\pm$ 0.00067 -0.00922 $\pm$ 0.00016 < 0.00057	$\Delta$ - $\sigma^2$ CrB	900101	00 01 00.003262 $\pm$ 0.000008	-00 21 16.03486 $\pm$ 0.00012	43.93 $\pm$ 0.10	0.32	23	$\sigma^2$ CrB (1611+343)	900101	16 14 41.067512 $\pm$ 0.000022 -0.021439 $\pm$ 0.000003 < 0.0000033	33 51 31.87419 $\pm$ 0.00029 -0.08666 $\pm$ 0.00005 < 0.00001	$\Delta$ -Cyg X1	910402	00 00 41.128564 $\pm$ 0.000022	01 33 37.89682 $\pm$ 0.00032	0.73 $\pm$ 0.30	0.59	7	Cyg X1 (1955+335)	910402	19 58 21.678600 $\pm$ 0.000101 -0.000309 $\pm$ 0.000014 < 0.0000093	35 12 05.84237 $\pm$ 0.00175 -0.00625 $\pm$ 0.00021 < 0.00015	$\Delta$ -HD199178	931017	-00 08 23.419214 $\pm$ 0.000017	-02 39 05.16806 $\pm$ 0.00026	8.59 $\pm$ 0.33	0.37	7	HD199178 (2100+468)	931017	20 53 53.636836 $\pm$ 0.000182 +0.002481 $\pm$ 0.000038 < 0.00017	44 23 11.08662 $\pm$ 0.00195 -0.00124 $\pm$ 0.00043 < 0.0014	$\Delta$ -AR Lac	920608	00 05 57.564529 $\pm$ 0.000026	03 27 51.77158 $\pm$ 0.00036	23.97 $\pm$ 0.37	0.66	9	AR Lac (BL Lac)	920608	22 08 40.855910 $\pm$ 0.000071 -0.004975 $\pm$ 0.000012 < 0.0000067	45 44 31.75156 $\pm$ 0.00094 +0.04703 $\pm$ 0.00019 < 0.0002	$\Delta$ -IM Peg	921201	-00 00 55.471694 $\pm$ 0.000025	00 41 34.93142 $\pm$ 0.00039	10.28 $\pm$ 0.62	0.38	3	IM Peg (3C454.4)	921201	22 53 02.276244 $\pm$ 0.000083 -0.001434 $\pm$ 0.000032 < 0.000027	16 50 28.49230 $\pm$ 0.00142 -0.02753 $\pm$ 0.00040 < 0.0015																																									
$\Delta$ -HR5110	930209	00 17 11.265295 $\pm$ 0.000031	02 45 40.82758 $\pm$ 0.00045	22.21 $\pm$ 0.45	1.38	27																																																																																																											
HR5110 (OP326)	930209	13 34 47.759476 $\pm$ 0.000040 +0.007154 $\pm$ 0.000011 < 0.0000013	37 10 56.76015 $\pm$ 0.00067 -0.00922 $\pm$ 0.00016 < 0.00057				$\Delta$ - $\sigma^2$ CrB	900101	00 01 00.003262 $\pm$ 0.000008	-00 21 16.03486 $\pm$ 0.00012	43.93 $\pm$ 0.10	0.32	23	$\sigma^2$ CrB (1611+343)	900101	16 14 41.067512 $\pm$ 0.000022 -0.021439 $\pm$ 0.000003 < 0.0000033	33 51 31.87419 $\pm$ 0.00029 -0.08666 $\pm$ 0.00005 < 0.00001	$\Delta$ -Cyg X1	910402	00 00 41.128564 $\pm$ 0.000022	01 33 37.89682 $\pm$ 0.00032	0.73 $\pm$ 0.30	0.59	7	Cyg X1 (1955+335)	910402	19 58 21.678600 $\pm$ 0.000101 -0.000309 $\pm$ 0.000014 < 0.0000093	35 12 05.84237 $\pm$ 0.00175 -0.00625 $\pm$ 0.00021 < 0.00015	$\Delta$ -HD199178	931017	-00 08 23.419214 $\pm$ 0.000017	-02 39 05.16806 $\pm$ 0.00026	8.59 $\pm$ 0.33	0.37	7	HD199178 (2100+468)	931017	20 53 53.636836 $\pm$ 0.000182 +0.002481 $\pm$ 0.000038 < 0.00017	44 23 11.08662 $\pm$ 0.00195 -0.00124 $\pm$ 0.00043 < 0.0014	$\Delta$ -AR Lac	920608	00 05 57.564529 $\pm$ 0.000026	03 27 51.77158 $\pm$ 0.00036	23.97 $\pm$ 0.37	0.66	9	AR Lac (BL Lac)	920608	22 08 40.855910 $\pm$ 0.000071 -0.004975 $\pm$ 0.000012 < 0.0000067	45 44 31.75156 $\pm$ 0.00094 +0.04703 $\pm$ 0.00019 < 0.0002	$\Delta$ -IM Peg	921201	-00 00 55.471694 $\pm$ 0.000025	00 41 34.93142 $\pm$ 0.00039	10.28 $\pm$ 0.62	0.38	3	IM Peg (3C454.4)	921201	22 53 02.276244 $\pm$ 0.000083 -0.001434 $\pm$ 0.000032 < 0.000027	16 50 28.49230 $\pm$ 0.00142 -0.02753 $\pm$ 0.00040 < 0.0015																																																				
$\Delta$ - $\sigma^2$ CrB	900101	00 01 00.003262 $\pm$ 0.000008	-00 21 16.03486 $\pm$ 0.00012	43.93 $\pm$ 0.10	0.32	23																																																																																																											
$\sigma^2$ CrB (1611+343)	900101	16 14 41.067512 $\pm$ 0.000022 -0.021439 $\pm$ 0.000003 < 0.0000033	33 51 31.87419 $\pm$ 0.00029 -0.08666 $\pm$ 0.00005 < 0.00001				$\Delta$ -Cyg X1	910402	00 00 41.128564 $\pm$ 0.000022	01 33 37.89682 $\pm$ 0.00032	0.73 $\pm$ 0.30	0.59	7	Cyg X1 (1955+335)	910402	19 58 21.678600 $\pm$ 0.000101 -0.000309 $\pm$ 0.000014 < 0.0000093	35 12 05.84237 $\pm$ 0.00175 -0.00625 $\pm$ 0.00021 < 0.00015	$\Delta$ -HD199178	931017	-00 08 23.419214 $\pm$ 0.000017	-02 39 05.16806 $\pm$ 0.00026	8.59 $\pm$ 0.33	0.37	7	HD199178 (2100+468)	931017	20 53 53.636836 $\pm$ 0.000182 +0.002481 $\pm$ 0.000038 < 0.00017	44 23 11.08662 $\pm$ 0.00195 -0.00124 $\pm$ 0.00043 < 0.0014	$\Delta$ -AR Lac	920608	00 05 57.564529 $\pm$ 0.000026	03 27 51.77158 $\pm$ 0.00036	23.97 $\pm$ 0.37	0.66	9	AR Lac (BL Lac)	920608	22 08 40.855910 $\pm$ 0.000071 -0.004975 $\pm$ 0.000012 < 0.0000067	45 44 31.75156 $\pm$ 0.00094 +0.04703 $\pm$ 0.00019 < 0.0002	$\Delta$ -IM Peg	921201	-00 00 55.471694 $\pm$ 0.000025	00 41 34.93142 $\pm$ 0.00039	10.28 $\pm$ 0.62	0.38	3	IM Peg (3C454.4)	921201	22 53 02.276244 $\pm$ 0.000083 -0.001434 $\pm$ 0.000032 < 0.000027	16 50 28.49230 $\pm$ 0.00142 -0.02753 $\pm$ 0.00040 < 0.0015																																																															
$\Delta$ -Cyg X1	910402	00 00 41.128564 $\pm$ 0.000022	01 33 37.89682 $\pm$ 0.00032	0.73 $\pm$ 0.30	0.59	7																																																																																																											
Cyg X1 (1955+335)	910402	19 58 21.678600 $\pm$ 0.000101 -0.000309 $\pm$ 0.000014 < 0.0000093	35 12 05.84237 $\pm$ 0.00175 -0.00625 $\pm$ 0.00021 < 0.00015				$\Delta$ -HD199178	931017	-00 08 23.419214 $\pm$ 0.000017	-02 39 05.16806 $\pm$ 0.00026	8.59 $\pm$ 0.33	0.37	7	HD199178 (2100+468)	931017	20 53 53.636836 $\pm$ 0.000182 +0.002481 $\pm$ 0.000038 < 0.00017	44 23 11.08662 $\pm$ 0.00195 -0.00124 $\pm$ 0.00043 < 0.0014	$\Delta$ -AR Lac	920608	00 05 57.564529 $\pm$ 0.000026	03 27 51.77158 $\pm$ 0.00036	23.97 $\pm$ 0.37	0.66	9	AR Lac (BL Lac)	920608	22 08 40.855910 $\pm$ 0.000071 -0.004975 $\pm$ 0.000012 < 0.0000067	45 44 31.75156 $\pm$ 0.00094 +0.04703 $\pm$ 0.00019 < 0.0002	$\Delta$ -IM Peg	921201	-00 00 55.471694 $\pm$ 0.000025	00 41 34.93142 $\pm$ 0.00039	10.28 $\pm$ 0.62	0.38	3	IM Peg (3C454.4)	921201	22 53 02.276244 $\pm$ 0.000083 -0.001434 $\pm$ 0.000032 < 0.000027	16 50 28.49230 $\pm$ 0.00142 -0.02753 $\pm$ 0.00040 < 0.0015																																																																										
$\Delta$ -HD199178	931017	-00 08 23.419214 $\pm$ 0.000017	-02 39 05.16806 $\pm$ 0.00026	8.59 $\pm$ 0.33	0.37	7																																																																																																											
HD199178 (2100+468)	931017	20 53 53.636836 $\pm$ 0.000182 +0.002481 $\pm$ 0.000038 < 0.00017	44 23 11.08662 $\pm$ 0.00195 -0.00124 $\pm$ 0.00043 < 0.0014				$\Delta$ -AR Lac	920608	00 05 57.564529 $\pm$ 0.000026	03 27 51.77158 $\pm$ 0.00036	23.97 $\pm$ 0.37	0.66	9	AR Lac (BL Lac)	920608	22 08 40.855910 $\pm$ 0.000071 -0.004975 $\pm$ 0.000012 < 0.0000067	45 44 31.75156 $\pm$ 0.00094 +0.04703 $\pm$ 0.00019 < 0.0002	$\Delta$ -IM Peg	921201	-00 00 55.471694 $\pm$ 0.000025	00 41 34.93142 $\pm$ 0.00039	10.28 $\pm$ 0.62	0.38	3	IM Peg (3C454.4)	921201	22 53 02.276244 $\pm$ 0.000083 -0.001434 $\pm$ 0.000032 < 0.000027	16 50 28.49230 $\pm$ 0.00142 -0.02753 $\pm$ 0.00040 < 0.0015																																																																																					
$\Delta$ -AR Lac	920608	00 05 57.564529 $\pm$ 0.000026	03 27 51.77158 $\pm$ 0.00036	23.97 $\pm$ 0.37	0.66	9																																																																																																											
AR Lac (BL Lac)	920608	22 08 40.855910 $\pm$ 0.000071 -0.004975 $\pm$ 0.000012 < 0.0000067	45 44 31.75156 $\pm$ 0.00094 +0.04703 $\pm$ 0.00019 < 0.0002				$\Delta$ -IM Peg	921201	-00 00 55.471694 $\pm$ 0.000025	00 41 34.93142 $\pm$ 0.00039	10.28 $\pm$ 0.62	0.38	3	IM Peg (3C454.4)	921201	22 53 02.276244 $\pm$ 0.000083 -0.001434 $\pm$ 0.000032 < 0.000027	16 50 28.49230 $\pm$ 0.00142 -0.02753 $\pm$ 0.00040 < 0.0015																																																																																																
$\Delta$ -IM Peg	921201	-00 00 55.471694 $\pm$ 0.000025	00 41 34.93142 $\pm$ 0.00039	10.28 $\pm$ 0.62	0.38	3																																																																																																											
IM Peg (3C454.4)	921201	22 53 02.276244 $\pm$ 0.000083 -0.001434 $\pm$ 0.000032 < 0.000027	16 50 28.49230 $\pm$ 0.00142 -0.02753 $\pm$ 0.00040 < 0.0015																																																																																																														

source of VLBI systematic error that might limit the accuracy of the measurement and might be reflected in the post-fit position rms is the varying structures of the reference sources that were not studied in details for each epoch of observations.

Only UX Ari observed over the longest duration, between 1983 and 1994, has an acceleration larger than 3 times the formal uncertainty. Upper limits to the absolute values of the accelerations are given for the other stars.

In order to test further the formal uncertainties of the VLBI astrometric parameters of Table 5, we have split the sets of observations of HR5110,  $\sigma^2$  CrB and Algol into two independent subsets since these three stars have been observed at many epochs; 16, 14 and 13 epochs, respectively. For HR5110, one subset is made of the 9 epochs of observations with the reference source OP326, separated by  $4.5^\circ$  from the star, and the other subset is made of 7 epochs of observations with the reference source 1338+381,  $1.5^\circ$  away. For  $\sigma^2$  CrB, one subset is made of the 7 epochs of observations when its flux density was larger than 10 milliJansky while the other subset is made of the 7 epochs with flux density smaller than 10 milliJansky. For Algol, the two subsets were made of 7 and 6 independent epochs chosen arbitrarily over the whole span of observations. The differences between these independent solutions are in Table 7, they are given in mas and mas/yr but also in units of the formal uncertainty ( $\sigma$ ) determined as the quadratic sum of the formal uncertainties of the two independent fits. For HR5110, the differences in right ascension and declination of Table 7 are largely due to the uncertainties of the ICRF coordinates of the two reference sources used: OP326 ( $\sigma_\alpha = 0.38$  mas,  $\sigma_\delta = 0.49$  mas) and 1338+381 ( $\sigma_\alpha = 1.65$  mas,  $\sigma_\delta = 1.20$  mas). The differences in  $\sigma$  of Table 7 show that the astrometric solutions are robust and that our formal uncertainties of the VLBI astrometric parameters are a good indication of the level of accuracy of the measurement for the three most observed stars of the program. Note that the astrometric solution of HR5110 in Table 5 is determined with all 16 epochs of observations since the coordinates of the two reference sources are consistent in the ICRF frame.

## 6. Discussion of individual stars

**LSI 61303.** (Star number in Hipparcos Input Catalogue: HIP 12469) is a massive main sequence Be star, a non-thermal radio source, an X-ray emitter and a  $\gamma$ -ray source identified as CG 135+01. Taylor & Gregory (1982) have discovered a 26.5 day periodicity in the radio emission variations of this object matching the periodicity in radial velocity measurements. This suggested that the Be star orbits an unseen companion that could be a neutron star accreting material from the Be star and forming an X-ray binary (White, 1989). A radio source size of 4.1 mas ( $1.4 \cdot 10^{14}$  cm) has been measured by VLBI at 1.6 GHz during quiescence (Lestrade et al. 1985) being 14 times larger than the separation of the binary determined by Hutchings & Cramp-ton (1981). Massi et al. (1993) have measured a smaller source size of 1–2 mas ( $3\text{--}6 \times 10^{13}$  cm) by VLBI at 5 GHz during an outburst and shown that the source is jet-like. Peracaula et

**Table 6.** Comparison between post-fit rms, VLBI systematic errors estimated in Sect. 4 and orbital jitters.

Star	Post-fit rms (mas)	VLBI Systematic errors (mas)	Orbital jitter rms (mas)
LSI61303	1.25	0.07	0.20
Algol	1.24	0.12	0.95
UX Ari	0.83	0.13	0.58
HR1099	0.84	0.28	0.52
HD283447	0.57	0.34	0.80
HR5110/OP326	1.33	0.54	0.40
HR5110/1338+381	0.53	0.18	0.29
$\sigma^2$ CrB	0.32	0.06	0.41
Cyg X1	0.59	0.19	0.10
HD199178	0.37	0.35	0.0
AR Lac	0.66	0.44	0.40
IM Peg	0.38	0.08	$\geq 0.39$

**Table 7.** Differences between the astrometric parameters determined from two independent sets of VLBI observations for  $\sigma^2$  CrB, HR5110 and Algol. The symbol  $\sigma$  is the quadratic combination of the uncertainties from the two adjustments.

	$\sigma^2$ CrB (mas, mas/yr)	HR5110 (mas, mas/yr)	Algol (mas, mas/yr)
$\Delta\alpha$	$0.27 = 1.0\sigma$	$2.02 = 1.4\sigma$	$0.76 = 0.6\sigma$
$\Delta\delta$	$0.25 = 1.0\sigma$	$1.18 = 1.1\sigma$	$0.66 = 0.6\sigma$
$\Delta\mu_\alpha$	$0.06 = 0.7\sigma$	$0.19 = 0.3\sigma$	$0.13 = 0.4\sigma$
$\Delta\mu_\delta$	$0.09 = 1.0\sigma$	$0.12 = 0.2\sigma$	$0.21 = 0.6\sigma$
$\Delta\pi$	$0.18 = 0.7\sigma$	$1.22 = 1.6\sigma$	$1.51 = 0.8\sigma$

al. (1998) reports a rapid expansion of the VLBI structure of LSI61303 during a small radio flare.

Phase-referenced VLBI observations have been conducted at 9 epochs between September 1989 and May 1995 and LSI 61303 was detected above 10 mJy at all epochs. The final astrometric adjustment has an rms for the post-fit position residuals of 1.25 mas which is relatively high compared to the plausible systematic error of 0.07 mas expected and the orbital jitter of 0.20 mas in Table 6. The jet-like structure of LSI61303 might be responsible for this relatively high post-fit residuals. Interestingly, this post-fit rms is comparable to the extent of the non-thermal radio emitting region (3 mas) expected for *in situ* acceleration of electrons in the enshrouding material around Cyg X3 and LSI61303 as proposed by Vestrand (1983).

An alternative explanation for the high positional jitter of the radio centroid of LSI61303 is scintillation since this star and its reference source 0241+622 are angularly close to the giant HII regions W3/W4/W5 (Goudis & White 1980). This complex region could provide a local screen in addition to the ionised interstellar medium of the Galaxy itself and be responsible for source broadening and refractive wandering at low frequency. It is also noticeable that the reference source 0241+622 is detected on US-continental baselines but is fully angularly resolved on

intercontinental VLBI baselines at 2.3 and 8.4 GHz (Jacobs 1995) as well as at 5 GHz while outbursts of LSI61303 are only partially angularly resolved on such baselines. This may imply that the local screens of the two sources separated by  $0.6^\circ$  are different, unless 0241+622 is intrinsically angularly large and resolved.

The small trigonometric parallax of LSI 61303 in Table 5 makes this star farther than 1.15 kpc when the upper limit of the uncertainty is included. This is consistent with the spectroscopic distance of 2.3 kpc from Gregory et al. 1979 but this is inconsistent with the Hipparcos trigonometric parallax of  $5.26 \pm 2.28$  milliarcsecond (The Hipparcos and Tycho Catalogues, European Space Agency, 1997, SP-1200, volume 5). However, Hipparcos data for this star cannot be fitted properly by neither a single nor a double star model (Froeschlé (1997) and Lindegren (1997)) and is flagged as a suspected non-single in the catalogue. The space velocity of LSI61303 relative to the solar system is  $58 \pm 5 \text{ km s}^{-1}$  based on the radial velocity of  $-55 \pm 4 \text{ km s}^{-1}$  (Hutchings & Crampton 1981) and on the transverse velocity of  $17 \pm 4 \text{ km s}^{-1}$  from our VLBI proper motion (Table 5) and assuming a distance of 2300 pc. This space velocity relative to the solar system is higher than the dispersion of star velocities ( $20 \text{ km s}^{-1}$ ). This is expected as the result of the supernova explosion kick if a neutron star lurks in the LSI 61303 system.

**Algol.** ( $\beta$  Per; HIP 14576) is a ternary system with a close binary B8V/K0IV (Orbit period = 2.86 days and semi-major axis = 2.2 mas) in a 1.86 year long period orbit with an A7m star (orbit semi-major axis = 94 mas) as described in Söderhjem (1980) for example. The long period orbit elements of Söderhjem (1980) have been confirmed by Pan et al. (1993) with high-precision Mark III optical interferometer observations at Mount Wilson.

Phase-referenced VLBI observations of Algol were conducted at 13 epochs from October 1984 to November 1994 and Algol was detected at all epochs with a flux density above 2 mJy. Our VLBI astrometric data cover more than five orbital revolutions of 1.86 years and clearly show an orbital motion of the radio emitting close binary that agrees with Söderhjem (1980) elements. In addition, we have been able to show on a finer angular scale that the radio emitting region is physically associated with the subgiant of the close binary at least over 2 consecutive orbital revolutions of 2.86 days in April 1989 (Lestrade et al. 1993a). Intriguingly, these 1989 VLBI observations show that the close binary orbital plane is approximately perpendicular to the long period orbital plane. In Table 5, we provide the VLBI position, proper motion and parallax of the mass center of the ternary system Algol by using the orbital elements of Söderhjem (1980) and the node for the close binary  $\Omega = 52^\circ$  of Lestrade et al. (1993a). The post-fit rms of this solution is 1.24 mas and the trigonometric parallax is  $\pi = 33.32$  mas. As a test, we have forced the short and long orbits to be coplanar with the same node  $\Omega = 132^\circ$  to make a 5-parameter astrometric fit and found that the adjustment to the VLBI data was not as good with a significantly higher post-fit rms of 2.19 mas. Hence, we confirm with our VLBI observations at 13 epochs the startling

result that the planes of the short and long orbits of the ternary system Algol are orthogonal as shown in Lestrade et al. (1993a) and initially discovered by optical polarimetry by Kempt et al. (1983).

We have found no significant acceleration in right-ascension and declination for Algol at the  $0.10 \text{ mas/yr}^2$  level. Our low VLBI proper motion of Algol corresponds to the transverse velocity  $V_T = \frac{a_0}{\pi} \sqrt{\mu_\alpha^2 \cos^2 \delta + \mu_\delta^2} = 0.38 \text{ km s}^{-1}$  and, if combined with the radial velocity  $V_R = +4.0 \pm 0.5 \text{ km s}^{-1}$  (Wilson 1953), it yields a close encounter of the solar system and Algol at the distance  $l_{enc} = \frac{1}{\pi} \sqrt{1 - \frac{V_R^2}{V_R^2 + V_T^2}} = 3 \pm 0.6 \text{ pc}$ , at the time  $t_{enc} = -\frac{a_0}{\pi} \frac{V_R}{V_R^2 + V_T^2} = -7.3 \pm 1 \times 10^6 \text{ years}$  ( $\pi$  is the parallax and  $a_0$  is the astronomical unit), when Algol is assumed to follow a straight line in space. At the time of closest encounter, Algol was 10 times closer to the solar system than it is now and its apparent magnitude was  $m_V = -2.8$ , or brighter than Sirius ( $m_V = -1.46$ ) as seen now in the night sky. Note that the life time of a B8V star is about 1 billion years.

Comparison with the FK5 astrometric parameters of Algol (FK5 star 111) yields the differences  $\Delta\alpha = 21 \pm 13 \text{ mas}$ ,  $\Delta\delta = 90 \pm 17 \text{ mas}$ ,  $\Delta\mu_\alpha = 1 \pm 0.5 \text{ mas/yr}$ ,  $\Delta\mu_\delta = 0.5 \pm 0.5 \text{ mas/yr}$ . Previous measurements of the trigonometric parallax of Algol are  $34 \pm 2 \text{ mas}$  by Bachman & Hershey (1975),  $35.46 \pm 1.1 \text{ mas}$  by Pan et al. (1993) and  $34.3 \pm 0.85 \text{ mas}$  by Gatewood et al. (1995). Our VLBI parallax ( $33.32 \pm 0.73 \text{ mas}$ ) is systematically lower by 0.3, 1.6 and 0.9 times the quadratically combined uncertainties of these other measurements done in the optical spectrum, respectively. The photocenter of the optical measurement is dominated by the brighter B8V star of the system while the radio measurements are tied to the corona of the subgiant K0. According to our tests, whether the 2.86-day orbital motion of the subgiant is included or not in the model, the VLBI parallax changes by no more than 0.5 mas. The final astrometric solution of Algol in Table 5 is based on a model including the 2.86-day orbit with the node  $\Omega = 52^\circ$ .

**UX Ari.** (HD21242; HIP 16042) is a very active close binary (G5V/K0IV,  $m=6.5$ ) of the RS CVn type with a period of 6.4 days and an orbit diameter  $a$  of 1.72 mas ( $a = \frac{a_1 \sin i + a_2 \sin i}{\sin i}$  with  $a_1 \sin i = 5.9 \cdot 10^6 \text{ km}$ ,  $a_2 \sin i = 5.3 \cdot 10^6 \text{ km}$  and  $i = 60^\circ$  in Carlos & Popper 1971). Phase-referenced VLBI observations of UX Ari were conducted at 12 epochs between July 1983 and May 1994 but the stellar system was below detectability at 2 epochs ( $S_{8.4GHz} \leq 3 \text{ mJy}$ ). The least-square-fit of the remaining 10 epochs between July 1983 and May 1994 provides the 7 astrometric parameters, including the acceleration of Table 5. Solving for the acceleration makes the post-fit position residual rms drop from 1.5 to 0.83 mas. The acceleration,  $-0.000041 \text{ s/yr}^2$  in right ascension ( $8\sigma$ ) and  $-0.00029''/\text{yr}^2$  in declination ( $4\sigma$ ), is much larger than the perspective secular change in the proper motion ( $1.2 \cdot 10^{-7}''/\text{yr}^2$  ( $V_R = 31 \text{ km s}^{-1}$ )). This acceleration could be caused by the presence of a companion gravitationally interacting with UX Ari and, if bound, the orbital period of this system should be many times our 11-year VLBI data span.

The largest systematic error expected for the relative coordinates between the extragalactic reference source 0326+277 and UX Ari is 0.13 mas in Table 6. This is much smaller than the rms of the post-fit position residuals (0.83 mas) which is more comparable to the orbital jitter (0.58 mas). One possibility is that the radio-emitting region is physically associated with one of the stellar components and tracks the orbital motion of the binary whose overall angular size is 1.72 mas. We studied the degree of correlation between the post-fit position residuals and the orbital motion projected on the sky with the elements of Carlos & Popper (1971) and the ephemerides of Landis et al. (1978). Preliminary results indicate that the radio emitting region might be associated with one of the stellar components.

The optical position of UX Ari in the FK5 system measured by Réquieme & Mazurier (1991) was compared to our VLBI position and the differences  $\Delta\alpha = 32$  mas and  $\Delta\delta = 5$  mas are significantly smaller than the dominant optical uncertainties (100 mas). Our VLBI parallax is also consistent with the value of 20 mas from van Altena as quoted in Johnston et al. (1985).

**HR 1099.** (V711 Tau; HIP 16846) is a very active close binary (G5IV/KIV) of the RS CVn type with a period of 2.837 days and an orbit diameter of 1.48 mas ( $a_1 \sin i = 2.4 \cdot 10^6$  km,  $a_2 \sin i = 1.9 \cdot 10^6$  km and  $i = 33^\circ$ ; Dorren & Guinan 1982; Fekel 1983). This close binary is part a visual binary ADS 2644A with an orbital period of 2101 years and an angular separation of  $6.2''$ .

Phase-referenced VLBI observations have been conducted at 8 epochs between March 1991 and May 1994 and HR 1099 was detected at all epochs above 2 mJy. The post-fit coordinate residual rms is 0.84 mas for the 5 astrometric parameter fit (Table 5) while plausible systematic errors are estimated to be 0.28 mas (Table 6) and the orbital jitter is 0.52 mas. Note that the orbital phases of the 8 epochs of observations are not uniformly distributed over the complete orbital period of the close binary, only ranging from phase  $\phi = 0.17$  radian to  $\phi = 0.66$  radian. Previous trigonometric parallaxes for HR 1099 are  $28 \pm 5$  mas from Jenkins (1952) and 32.8 mas from Van Altena as quoted in Johnston et al. (1985) to be compared to  $33.9 \pm 0.5$  mas with our VLBI observations. HR 1099 is a candidate guide star for the Gravity Probe B mission.

**HD283447.** (V773 Tau, HIP 19762) is a weak-lined T Tauri of spectral type K3 (PMS) in the Taurus-Auriga star forming region that exhibits highly variable non-thermal radio emission. Ghez et al. (1993) found a companion at  $a = 112$  mas and P.A. =  $295^\circ$  by IR speckle imaging. Welty (1995) discovered that HD283447 is really a spectroscopic binary with a period of 51.075 days and an orbit diameter of 2.5 mas ( $a_1 \sin i = 22.1 \cdot 10^6$  km,  $a_2 \sin i = 29.2 \cdot 10^6$  km,  $i = 66^\circ$ ). The structure of the radio emitting region in HD283447 can change morphology and evolves from an ultra-compact to an extended source of 24–30 stellar radii (2.6 mas) comparable to the diameter of the orbit, as shown with VLBI visibility functions by Phillips et al. (1991). Recently, HD283447 was mapped by VLBI and found to exhibit a structure with two components separated by the distance between the two stellar components predicted by the Welty 1995 ephemerides (Phillips et al. 1996).

Phase-referenced VLBI observations were conducted at 9 epochs between September 1992 and September 1994 and HD283447 was detected above 2 mJy at all epochs. The first observation (92 Sept 11) was conducted with the extragalactic reference source 0400+258 (separation from HD283447 =  $3.3^\circ$ ) and subsequent observations with the reference source 0405+304 (separation  $2.9^\circ$ ). The post-fit coordinate residual rms is 0.57 mas and is smaller than the combination of the plausible systematic error 0.34 mas and the orbital jitter 0.80 mas (Table 6) implying that the centroid of the radio-emission is in the intra-stellar region.

The determination of the precise trigonometric parallax of HD283447 ( $\pi = 6.74 \pm 0.25$  mas) with our VLBI observations is important because it provides the first directly measured distance to the nearby star forming region Taurus-Auriga of  $148 \pm 5$  pc. This VLBI trigonometric distance is consistent with the estimate of  $140 \pm 10$  pc by optical spectrophotometry (Kenyon et al. 1994) while the generally assumed distance to Taurus-Auriga is 160 pc.

**HR5110.** (HIP 66257) is an active semi-detached binary (F2IV/K2IV) with properties akin to both the RS CVn and Algol types. It has a period of 2.6 days and an orbit diameter of 0.97 mas ( $a_1 \sin i = 0.4 \cdot 10^6$  km,  $a_2 \sin i = 0.74 \cdot 10^6$  km and  $i = 10^\circ$ ; Eker & Doherty 1987).

Phase-referenced VLBI observations were conducted at 16 epochs from May 1987 to May 1994 and HR5110 was detected at all epochs with a flux density above 2 milliJansky. The 5 astrometric parameters of HR5110 fitted on the 15 epochs of observations are in Table 5 and the post-fit coordinate residual rms is 1.38 mas. We used two extragalactic reference sources in the course of our program. Originally, we used OP326 separated by  $4.5^\circ$  from HR5110 until September 1992 when the extragalactic radio source 1338+381 in Patnaik et al. (1992) appeared to be a better choice because it is closer to HR5110 with an angular separation of  $1.5^\circ$ . However, 1338+381 is a compact double (Bouchy et al. 1998) and its structure limits the astrometric precision, if not accounted for. We used 1338+381 as a reference source after September 1992, except in May 1994 when we conducted observations with both reference sources for verification. Structure corrections for 1338+381 have been computed in Bouchy (1995). The astrometric parameters have been determined by using the 2 independent series of observations conducted relative to OP326 and 1338+381. The differences are in Table 7 and show that the solution is robust and that the formal uncertainties should be indicative of the accuracy of the measurement.

A preliminary astrometric solution for HR5110 was reported earlier in Lestrade et al. (1993b) and was based on only 4 VLBI epochs yielding a trigonometric parallax of 14 mas. An interferometric ambiguity in the measured coordinates at one of the four epochs caused this erroneous result. Our larger and redundant sets of measurements now with 16 epochs of observations make it impossible that an ambiguity could remain undetected.

Comparison with the optical FK5-based position of HR5110 by Réquieme & Mazurier (1991) yields  $\Delta\alpha = -2$  mas ( $0.0\sigma$ ),  $\Delta\delta = -51$  mas ( $0.5\sigma$ ) and direct comparison to the FK5

(HR5110 = FK5 star 502) yields  $\Delta\alpha = -36$  mas ( $2.2\sigma$ ),  $\Delta\delta = 3$  mas ( $0.1\sigma$ ),  $\Delta\mu_\alpha = 0.2$  mas/yr ( $0.3\sigma$ ),  $\Delta\mu_\delta = 0.3$  mas/yr ( $0.5\sigma$ ). The differences found in  $\alpha$  and  $\delta$  for HR5110 but also for Algol and UX Ari above demonstrate that the ICRF VLBI celestial frame is globally aligned on the FK5 to better than 100 mas. The optical trigonometric parallax of Jenkins (1952) is  $19 \pm 6$  mas and is consistent with our determination ( $22.2 \pm 0.4$  mas). HR5110 is a candidate guide star for the NASA Gravity Probe B space mission and the formal precision of our VLBI proper motion, 0.16 mas/yr, is very close to the mission requirement of 0.15 mas/yr.

$\sigma^2$  CrB. (HIP 79607) is a close binary (detached) of the RSCVn type with two chromospherically active main sequence stars (F6V/G0V) with a period of 1.14 days and an orbit diameter of 1.30 mas ( $a_1 \sin i = 0.99 \cdot 10^6$  km,  $a_2 \sin i = 1.02 \cdot 10^6$  km and  $i = 28^\circ$ ; (Bakos 1984)). This close binary is part of a visual binary ADS 9979A with an orbital period of 1000 years and an angular separation of  $6.4''$ .

Phase-referenced VLBI observations of  $\sigma^2$  CrB were conducted at 14 epochs between May 1987 and November 1994 relative to the reference source 1611+343 (DA406) which is a 2 Jy quasar only  $0.5^\circ$  away from  $\sigma^2$  CrB. The star was detected at all epochs above 3 mJy. The 5 fitted astrometric parameters are in Table 5 and the rms of the post-fit residuals is 0.32 mas. This rms can be compared to the plausible systematic error of 0.06 mas and to the orbital jitter of 0.41 mas of Table 6. Similarly to HD283447, preliminary results indicate that the averaged position of the radio emitting region is in the intra-system region (see also Lestrade 1996).

The formal precision of the astrometric parameters (0.12 mas in  $\Delta\alpha$  and  $\Delta\delta$ ; 0.05 mas/yr for the proper motion components and 0.1 mas for the trigonometric parallax) is unprecedented in stellar astrometry except for millisecond pulsar timing astrometry. For example, the formal precision of the trigonometric parallax is 10 times better than the precision from the HIPPARCOS mission. This makes the actual accuracy of our determination difficult to assess. We have attempted to estimate it by testing for the robustness of the solution in splitting the data into 2 subsets of 7 independent epochs. The differences between the two solutions are in Table 7 and are all at the  $1\sigma$  level or less and this attests of the robustness of the solution. Another verification is to compare the astrometric parameters of  $\sigma^2$  CrB determined with the 14 epochs of observations with the ones reported earlier in Lestrade et al. (1992) based on only the first 4 epochs. Allowing for the improvements in the coordinates of the reference source 1611+343 in the ICRF VLBI reference frame, the differences for  $\sigma^2$  CrB are  $\Delta\alpha = 0.25 \pm 0.30$  mas,  $\Delta\delta = 0.03 \pm 0.30$  mas,  $\Delta\mu_\alpha = 1.83 \pm 0.18$  mas/yr,  $\Delta\mu_\delta = 0.54 \pm 0.20$  mas/yr,  $\Delta\pi = 0.30 \pm 0.20$  mas. These differences are acceptable when compared to the combined uncertainties except for the  $10\sigma$  discrepancy for proper motion in right-ascension. The early solution for  $\sigma^2$  CrB was based on 4 epochs spanning 2 years only and one epoch (1988 November 27) was a marginal detection causing the discrepancy in  $\mu_\alpha$ . This marginal detection has been removed from our final data set. If it is removed also from the earlier solution (which be-

comes now a 3-epoch solution with 1 degree of freedom) the discrepancy in  $\mu_\alpha$  is reduced to  $3\sigma$  and the other differences are similar to the ones above. This is another strong indication of the robustness of the solution. The differences of our VLBI position with the FK5-based position of Réquieme & Mazurier (1991) are  $\Delta\alpha = 75$  mas ( $0.8\sigma$ ) and  $\Delta\delta = 81$  mas ( $0.8\sigma$ ).

**Cyg X1.** (HIP 98298) is a X-ray binary with a supergiant O9.7Iab possibly in orbit around a black hole with an orbital period of 5.6 days.

Phase-referenced VLBI observations have been conducted at 7 epochs between March 1988 and November 1993 and Cyg X1 was detected at all epochs above its quiescent level of 10 mJy. The final fit in Table 5 with the post-fit residual rms of 0.59 mas includes only 6 epochs because of an anomalously large residual ( $-2.49$  mas in  $\alpha$  and 0.8 mas in  $\delta$ ) on August 24 1992 that lead us to discard this epoch of observation. Systematic error is estimated to be 0.19 mas and the orbital jitter is 0.1 mas (Table 6). Refractive scintillation in the ionised interstellar medium should be negligible at the observing frequency of 8.4 GHz.

The residual rms of 0.59 mas corresponds to a scale length of  $\sim 2 \cdot 10^8$  km at the distance of 2000 pc. This is much larger than the binary system size ( $4 \cdot 10^7$  km) and might be an indication that *in situ* acceleration of electrons of the enshrouding matter as proposed by Vestrand (1983) for LSI61303 applies also to Cyg X1. The large position residual on August 24 1992 corresponds to a scale length of  $9 \cdot 10^8$  km and might be an extreme event where a major burst of energetic electrons occurred within the large enshrouding envelope, relatively far from the binary.

The trigonometric parallax determined is  $0.73 \pm 0.30$  mas (Table 5), or  $1400_{-400}^{+900}$  pc. This is consistent with the distance of 2000 pc generally assumed for Cyg X1 and based on its spectral type. The space velocity of Cyg X1 relative to the solar system is  $70 \pm 3$  km s $^{-1}$  (optical distance 2000 pc) or  $50 \pm 2$  km s $^{-1}$  (VLBI distance 1400 pc) with our VLBI proper motion and the radial velocity of  $-13 \pm 2.5$  km s $^{-1}$  (Wilson 1953). The higher space velocity is consistent if one of the components of the system being a black hole or a neutron star, similarly to LSI 61303.

**HD199178.** (HIP 103144) is an extremely fast rotating single late-type giant with a photometric rotation period of 3.33 days and  $v \sin i$  of 80 km s $^{-1}$  (Huenemoerder 1986). It might be an FK Com type star.

Phase-referenced VLBI observations have been conducted at 8 epochs between September 1992 and September 1994 and HD199178 was detected at all but 2 epochs when its flux density was  $\leq 4$  milliJansky. The 5 astrometric parameter fit in Table 5 has been done with the 6 remaining epochs and the post-fit residual rms is 0.37 mas, comparable to the plausible systematic error of Table 6.

The distance  $116 \pm 4$  pc determined from our VLBI observations improves on the range 90 to 140 pc generally used for this interesting star. A large outburst of 300 mJy occurred on 1994 May 14 and corresponds to the very high radio luminosity of  $10^{18.7}$  ergs/s/Hz for a radio star. The flux density was so high

that the 10-hour observations were split into 1-hour segments and a position was measured for each segment. This analysis provides evidence for a motion of the radio emitting region at constant velocity of  $1500 \text{ km s}^{-1}$  over a distance as large as 7 radii of HD199178 ( $1R_* = 5R_\odot$ ). This is reminiscent of coronal mass ejection on the Sun at similar speed and distance. This result will be reported in detail elsewhere.

**AR Lac.** (HIP 109303) is an eclipsing close binary (G2IV/K0IV) of the RS CVn type with a period of 1.98 days and an orbit diameter of 1.00 mas ( $a_1 \sin i = 3.17 \cdot 10^6 \text{ km}$ ,  $a_2 \sin i = 3.15 \cdot 10^6 \text{ km}$  and  $i = 87^\circ$ ).

Phase-referenced VLBI observations have been conducted at 7 epochs between April 1989 and May 1994 and AR Lac was detected at all epochs above 2 mJy. The post-fit residual rms is 0.66 mas for the 5 astrometric parameter fit in Table 5. If the observation on July 1<sup>st</sup> 1990 is ignored, the post-fit residual rms for the 6 remaining observations drops considerably to 0.39 mas. The VLBI array used for this epoch (July 1990) was reduced to DSS14, OVRO and Pie Town and provided a poor u-v coverage and relatively short baselines. However, if this residual ( $-1.0 \text{ mas}$  in  $\alpha$ ;  $-1.3 \text{ mas}$  in  $\delta$ ) is real, the centroid of the radio emission, which was not particularly strong during the observation, would have moved by  $\sim 1.5$  times the separation of the binary system or 5 times the radius of the subgiant K0 with respect to the averaged position. This observation was kept in the fit that yielded the astrometric parameters of AR Lac in Table 5 because the parameters change by less than  $1\sigma$ . The distance of AR Lac was between 40 and 50 pc before our VLBI determination of  $41.7 \pm 0.6 \text{ pc}$ .

**IM Peg.** (HIP 112997) is a single line spectroscopic binary (K1 III) of the RS CVn type with a period of 24.649 days. The semi-major axis of the giant orbit  $a_1$  is 0.09 mas ( $a_1 \sin i = 0.98 \cdot 10^6 \text{ km}$  and  $i = 60^\circ$ ; Poe & Eaton, 1985; Eaton et al. 1983). Phase-referenced VLBI observations were conducted at 7 epochs between December 1991 and July 1994 but IM Peg was detected above 2 mJy at 4 epochs only. The rms of the post-fit residuals is 0.38 mas for the 5 astrometric parameter fit in Table 5. This rms can be compared to the small systematic error of 0.08 mas in Table 6 expected for this close pair. Only a lower bound is set on the orbital jitter by  $a_1$ . The distance to IM Peg was only approximatively known (50 pc in Majer et al. (1986)) and is now  $97 \pm 6 \text{ pc}$  with our VLBI determination. IM Peg is a candidate guide star for the Gravity Probe B mission and its proper motion with an uncertainty of 0.40 mas/yr must be improved to reach the 0.15 mas/yr required by the mission. Note that the time spanned by the observations is only 3 years and new observations of the same quality acquired in 1997 should reduce this uncertainty by a factor of 2.

## 7. Conclusion

Multiple epoch phase-referenced VLBI observations of 11 radio emitting stars with flux densities as low as a few mJy have yielded relative positions, proper motions and trigonometric parallaxes with formal uncertainties smaller than 1 milliarcsecond. Applications of high-precision astrometry of radio weak

sources include measurement of proper motions and trigonometric parallaxes of pulsars, searches for extra-solar planets and brown dwarfs, and, more generally, unseen companions around radio-emitting stars and localisation of the radio-emitting regions in binary systems.

*Acknowledgements.* We acknowledge the strenuous efforts by the staffs of the participating observatories of the NASA Deep Space Network, the US VLBI network, the NRAO VLBA network and the European VLBI Network and of the VLBI Processor at Haystack to support the many hours of observation and correlation for this program. We are grateful to Pam Wolken for her constant attention to our program on the Deep Space Network. Maria Rioja acknowledges support for her research by the European Union under contract CHGECT920011. The National Radio Astronomy Observatory (NRAO) is operated by Associated University, Inc., under cooperative agreement with the National Science Foundation. The research described in this report was carried out, in part, at the Jet Propulsion Laboratory, California Institute of Technology, under contract with the National Aeronautics and Space Administration.

## References

- Bakos, G.A., 1984, AJ 89, 1740–1744
- Boucher, C., Altamimi, Z., Duhem, L., 1993, IERS Technical Note 15, Observatoire de Paris, France
- Bouchy, F., 1995, DEA Memorandum June 1995, Observatoire de Paris, p.33
- Bouchy, F., Lestrade, J.-F., Ransom, R.R., et al., 1998, A&A 335, 145–151
- Bachman, P.J., Hershey, J.L., 1975, AJ 80, 836–843
- Carlos, R.C., Popper, D.M., 1971, PASP 83, 504
- Charlot, P., 1990, AJ 99, 1309–1326
- Collins, C.B., Hawking, S.W., 1973, MNRAS 162, 307
- Dorren, J.D., Guinan, E.F., 1982, ApJ 252, 296–301
- Dulk, G.A., 1985, Ann. Rev. A&A 23, 169
- Eaton, J.A., Hall, D.S., Henry, G.W., et al., 1983, Ap. Space Science 89, 53
- Eker, Z., Doherty, L.R., 1987, MNRAS 228, 869–881
- Eubanks, T.M., Archinal, B.A., Carter, M.S., et al., 1991, IERS Technical Note n 8, IERS, Observatoire de Paris, France, p.73–79
- Fekel, F.C., 1983, ApJ 268, 274–281
- Froeshlé, M., Kovalevsky, J., 1982, A&A 116, 89
- Froeschlé, M., 1997, private communication
- Gatewood, G., Stein, J., Joost Kiewiet de Jonge, T., Persinger, T., Reiland, 1992, AJ 104, 1237
- Gatewood, G., De Jonge, J.K., Heintz, W.D., 1995, AJ 109, 434–439
- Ghez, A.M., Neugebauer, G., Matthews, K., 1993, AJ 106, 2005
- Goudis, L., White N.J., 1980, A&A 83, 79
- Gregory, P.C., Taylor A.R., Crampton, D., et al., 1979 1979, AJ 84, 1030
- Huenemoerder, D.P., 1986, AJ 92, 673
- Hummel, C.A., Armstrong, J.T., Buscher, D.F., Mozurkewich, D., Quirrenbach, A., Vivekanand, M., 1995, AJ 110, 376–390
- Hutchings, J.B., Crampton, D., Glaspey, J., Walker, G.A.A., 1973, ApJ 182, 549
- Hutchings, J.B., Crampton, D., 1981, PASP 93, 486
- Jacobs, C.S., 1995, private communication
- Jenkins L.F., 1952 (and 1963), General Catalogue of Trigonometric Parallaxes

- Johnson, K.J., Wade, C.M., Florkowski, D. R., de Veigt, C., 1985, *AJ* 90, 1343
- Johnston, K.J., Fey, A.L., Zacharias, N., et al. 1995, *AJ* 110, 880–915
- Kempton, J.C., Henson, G.D., Barbour, M.S., Kraus, D.J., Collins, G.W., 1983, *ApJ* 273, L85
- Kenyon, S.J., Dobrzycka, D., Hartmann, L., 1994, *AJ* 108, 1872–1880
- Klobuchar, J.A., 1975, AFCRL-TR-75-0502 (NTIS ADA 018862)
- Kovalevsky, J., Lindegren, L., Froeschlé, M., et al., 1995, *A&A* 304, 34–43
- Landis, H.J., Lovell, L.P., Hall, D.S., Henry, G.W., Renner, T.R., 1978, *AJ* 83, 176
- Lestrade, J-F., Preston, R.A., Slade, M.A., 1982, in “Very Long Baseline Interferometry Techniques”, edited by F. Biraud, (Editions Cepadues), p. 199
- Lestrade, J-F., Mutel, R.L., Preston, R.A., Phillips, R.B., 1985, in *Radio Stars* (Astrophysics and Space Science Library, volume 116) edited by R.M. Hjellming and D.M. Gibson, (Reidel: Dordrecht), 275
- Lestrade, J.-F., Rogers, A.E.E., Whitney, A.R., et al., 1990, *AJ* 99, 1663
- Lestrade, J.-F., Phillips, R.B., Preston, R.A., Gabuzda, D.C., 1992, *A&A* 258, 112–115
- Lestrade, J.-F., Phillips, R.B., Hodges, M.W., Preston, R.A., 1993a, *ApJ* 410, 808–814
- Lestrade, J-F, Phillips, R.B., Jones, D.L., Preston, R.A., Gabuzda, D., 1993b, in “Sub-arcsecond Radio Astronomy”, edited R.J. Davis and R.S. Booth, (Cambridge University), p. 415–417
- Lestrade, J.-F., Jones, D.L., Preston, R.A., et al., 1995, *A&A* 304, 182–188
- Lestrade, J.-F., 1996, in *Proceedings of IAU Symp 176 on Stellar Surface Structure*, Vienna, October 1995, edited by K. Strassmeier and J.L. Linsky, Published by Kluwer Ac. Pub., p. 173–180
- Lindegren, L., Kovalevsky, J., 1995, *A&A* 304, 189–210
- Lindegren, L. 1997, private communication.
- Ma, C., Arias, F., Eubanks, T.M., et al., 1998, *AJ* 116, 516
- Ma, C., Shaffer, D.B., de Veigt, C., Johnston, K.J., Russell, J.L., 1990, *AJ* 99, 1284–1298
- Massi, M., Paredes, J.M., Estalella, R. Felli, M., 1993, *A&A* 269, 249
- Majer, P., Schmitt, J.H.M., Golub, L., Harnden, F.R., Rosner, R., 1986, *ApJ* 300, 360–373
- Monet D.G., Dahn, C.C., Vrba, F.J., et al., 1992, *AJ* 103, 638–665
- Pan, X., Shao, M., Colavita, M.M., 1993, *ApJ* 413, L129
- Patnaik, A.R., Browne I.W.A., Wilkinson, P.N., Wrobel, J.R., 1992, *MNRAS* 254, 655–676
- Peracaula, M., Gabuzda, D.C., Taylor, A.R., 1998, *A&A* 330, 612–618
- Perryman, M.A.C., Lindegren, L., Kovelevskiy, J., et al., 1995, *A&A* 304, 69
- Perryman, M.A.C., 1989, *Nature* 340, 111–116
- Phillips, R.B., Lonsdale, C.J., Feigelson, E.D., 1991, *ApJ* 382, 261–269
- Phillips, R.B., Lonsdale, C.J., Feigelson, E.D., Deeney, B.D., 1996, *ApJ* 111, 918
- Poe, C.H., Eaton, J.A., 1985, *ApJ* 289, 644–659
- Rogers, A.E.E., Cappallo, R.J., Hinteregger, H.F., 1983, *Science* 219, 51
- Rogers, A.E.E., 1989, in “Gravitational Lenses”, edited by J.M. Moran, J.N. Hewitt, K.Y. Lo, (Springer: Berlin), 77
- Requiem, Y., Mazurier, J.M., 1991, *A&AS* 89, 311–318
- Saastamoinen, J., 1973, *Bull. Géodésique* 105, 279
- Shapiro, I.I., Wittels, J.J., Counselman I.I.I., et al., 1979, *AJ* 84, 1459
- Strassmeier, K.G., et al., 1988, *A&AS* 72, 291–345
- Söderhjelm, S., 1980, *A&A* 89, 100
- Sovers, O.J., 1991, *NASA JPL TDA Progress Report* 42–106, Aug 15, 1991, pp. 364–383
- Sovers, O.J., Jacobs, C.S., 1996, *JPL Publication* 83–39, revision 6, (Pasadena:JPL)
- Taylor, A.R., Gregory, P.C., 1982, *ApJ* 255, 210
- Taylor, A.R., Kenny, H.T., Spencer, R.E., Tzioumis, A., 1992, *ApJ* 395, 263
- Tinney, C.G., 1993, *AJ* 105, 1169
- van de Kamp, P., 1981, *Stellar Path*, *Astr. and Sp. Science Library*, vol. 85, Reidel Publish.
- Vestrand, W.T., 1983, *ApJ* 271, 304
- Welty, A. D., 1995, *AJ* 110, 776
- White, N.E., 1989, *A&AR* 1, 85
- Wilson, R.E., 1953, *General Catalogue of Stellar Radial Velocities*, Carnegie Institution of Washington, Publication 601